REPUBLIC OF TURKEY
YILDIZ TECHNICAL UNIVERSITY
GRADUATE SCHOOL OF NATURAL AND APPLIED SCIENCES

ENERGY MANAGEMENT ON PARALLEL HYBRID ELECTRICAL VEHICLES

Turgay GÜCÜKOĞLU

MASTER OF SCIENCE THESIS
Department of Control and Automation Engineering
Program of Control and Automation Engineering

Advisor
Asst. Prof. Dr. Levent UCUN

July, 2019

REPUBLIC OF TURKEY
YILDIZ TECHNICAL UNIVERSITY
GRADUATE SCHOOL OF NATURAL AND APPLIED SCIENCES

ENERGY MANAGEMENT ON PARALLEL HYBRID ELECTRICAL VEHICLES

A thesis submitted by Turgay GÜCÜKOĞLU in partial fulfillment of the requirements for the degree of **MASTER OF SCIENCE** is approved by the committee on 11.07.2019 in Department of Control and Automation Engineering, Program of Control and Automation Engineering .

Asst. Prof. Dr. Levent UCUN
Yildiz Technical University
Advisor

Approved By the Examining Committee

Asst. Prof. Dr. Levent UCUN, Advisor
Yildiz Technical University

Prof. Dr. Şeref Naci ENGİN, Member
Yildiz Technical University

Asst. Prof. Dr. İlker ÜSTOĞLU, Member
İstanbul Technical University

I hereby declare that I have obtained the required legal permissions during data collection and exploitation procedures, that I have made the in-text citations and cited the references properly, that I haven't falsified and/or fabricated research data and results of the study and that I have abided by the principles of the scientific research and ethics during my Thesis Study under the title of Energy Management on Parallel Hybrid Electrical Vehicles supervised by my supervisor, Asst. Prof. Dr. Levent UCUN. In the case of a discovery of false statement, I am to acknowledge any legal consequence.

Turgay GÜCÜKOĞLU

Signature

Dedicated to my family

ACKNOWLEDGEMENTS

Firstly, I would like to express my very great appreciation to previous supervisor Prof. Dr. İbraim B. Küçükdemiral and current supervisor Asst. Prof. Dr. Levent Ucun for their continuous support, patience, useful comments and encouragement during this study.

I would like to thank my colleagues Ahmet Sakallı, Ahmet Can Erdem, Dr. Koray Erhan, Mani Kazimi, Emre Zengin from AVL Research and Engineering Turkey for their motivational talks and guidance. They have never denied my help request even if they are fully loaded with urgent tasks.

I would like to express my appreciation to my parents for their support throughout my life.

Finally, I would like to express my deepest gratitude to my wife whose strong love, huge patience, unconditional encouragement and support are endless. I dedicate this work to my sweetheart wife Aylin Gücükoğlu and my lovely daughter Evrim Gücükoğlu.

Turgay GÜCÜKOĞLU

TABLE OF CONTENTS

LIST OF SYMBOLS

A	Vehicle Frontal Area
a	Parameter Limiting Factor of The Search Space
a_v	Vehicle Acceleration
c_d	Drag Coefficient
c_r	Rolling Resistance Coefficient
D_b	Brake Actuator Bore Diameter
F_{net}	Total Traction Force
F_a	Aerodynamic Drag Force
F_g	Gravitational Force due to Road Slope
F_r	Wheel Rolling Resistance Force
g	Gravitational Acceleration
I_b	Battery Current
J	Main Cost Function Value of Optimization Strategy
J_i	Cost Function Value of Particular Point
J_m	Electric Motor Inertia
J_w	Total Inertia of Wheels
J_{pt}	Equivalent Inertia of Vehicle
k	Iteration Step
m_{CO2}	Mass of Emitted CO_2
m_{fuel}	Mass of Consumed Fuel
m_v	Vehicle Mass
N	Population Dimension in Big Bang phase
N_{brake}	Number of Brakes

N_{pads}	Number of Brake Pads on Each Wheel
n_g	Gear Ratio
P	Applied Brake Pressure
P_m	Mechanical Output Power of Motor
R_i	Cell Internal Resistance
R_m	Mean Radius of Brake Pad Force Application on Brake Rotor
r_w	Wheel Radius
r	Random Number
SOC_{in}	Initial SOC of Battery
T_b	Brake Torque on Wheels
T_d	Torque Demand Sent to Traction Block in Hybrid Control System
T_e	Engine Torque
T_m	Motor Torque
T_{net}	Total Net Torque
T_s	Instant Traction Torque Capability of Vehicle System
u	Control Input
U_b	Cell Terminal Voltage
U_{oc}	Cell Open Circuit Voltage
v	Vehicle Velocity
X_c	Center of Mass
X_i	Particular Position Within n-dimensional Search Section
α	Fuzzy-PID Output Porpotional Gain
β	Fuzzy-PID Output Integral Gain
ε	Controller Input Error
ϑ_{actual}	Instant Speed of Vehicle
ϑ_{ref}	Speed Reference
μ_g	Gear Box Efficiency
μ_k	Disc Pad-Rotor Coefficient of Kinetic Friction
ρ_{air}	Air Density

σ	Weighted Coefficient of Consumed Fuel
φ_A	Acceleration Pedal Position Rate
φ_B	Brake Pedal Position Rate
ω_e	Engine Rotational Speed
ω_g	Gearbox Input Shaft Speed
ω_m	Motor Rotational Speed
ω_w	Wheel Rotational Speed

LIST OF ABBREVIATIONS

AP	Acceleration Pedal
BBBC	Big Bang-Big Crunch
BP	Brake Pedal
BWS	Batery Working State
C-PID	Conventional PID controller
DP	Dynamic Programming
DIP	Driver’s Intention Predictor
ECMS	Equivalent Consumption Minimization Strategy
eMotor	Electric Motor
EV	Electric Vehicle
FLC	Fuzzy Logic Controller
F-PID	Fuzzy-PID controller
GA	Genetic Algorithm
HEV	Hybrid Electric Vehicle
HWFET	Highway Fuel Economy Cycle
ICE	Internal Combustion Engine
MF	Membership Function
MPC	Model Predictive Control
OCV	Open Circuit Voltage
QP	Quadratic Programming
PBC	Power Balance Controller
PMP	Pontryagin’s Minimum Principle
RL	Reinforcement Learning

SMC	State Machine Control
SOC	State of Charge

LIST OF FIGURES

LIST OF TABLES

ABSTRACT

Energy Management on Parallel Hybrid Electrical Vehicles

Turgay GÜCÜKOĞLU

Department of Control and Automation Engineering
Master of Science Thesis

Advisor: Asst. Prof. Dr. Levent UCUN

Many researches regarding to optimization of power and energy consumption in hybrid electric vehicles to reduce fuel-rate and emission parameters have been made for years. As a summary, applied methods are classified into two major groups: rule-based and optimization-based. There are many types of application under these groups such as Traction Mode Transition Control, Fuzzy Logic, Model Predictive Control (MPC), etc.

In this study, it is aimed to apply a new energy management optimization method for parallel-hybrid electric vehicles. Big bang-big crunch optimization (BBBC) as new strategy is chosen for tuning Fuzzy-PID controller and conventional-PID parameters. Firstly, controllers and method are integrated to selected parallel hybrid vehicle drivetrain for simulation. Then, F-PID and conventional-PID parameters are tuned by BBBC to find minimum error between speed reference and vehicle actual velocity considering fuel consumption. Results indicate that Fuzzy-PID control leads to lower fuel-rate [L/100km] as it is compared to conventional-PID controller.

Keywords: Energy management, parallel-hybrid electric vehicle, big bang-big crunch optimization, fuzzy-PID

YILDIZ TECHNICAL UNIVERSITY
GRADUATE SCHOOL OF NATURAL AND APPLIED SCIENCES

ÖZET

Paralel Hibrit Elektrikli Araçlarda Enerji Yönetimi

Turgay GÜCÜKOĞLU

Kontrol ve Otomasyon Mühendisliği Anabilim Dalı
Yüksek Lisans Tezi

Danışman: Dr. Öğr. Üyesi Levent UCUN

Hibrit elektrikli araçlarda yakıt oranını ve emisyon parametrelerini azaltmak için güç ve enerji tüketimini optimize etmeye yönelik birçok araştırma yıllardır yapılmıştır. Özet olarak, uygulanan yöntemler kural temelli ve optimizasyon temelli olmak üzere iki ana gruba ayrılır. Bu gruplar altında Çekiş Modu Geçiş Kontrolü, Bulanık Mantık, Model Tahmini Kontrolü (MPC) vb. birçok uygulama tipi vardır.

Bu tez çalışmasında, paralel hibrit elektrikli araçlar için yeni bir enerji yönetimi optimizasyon yöntemi uygulanması amaçlanmıştır. Bulanık Mantık-PID kontrolörü ve geleneksel-PID kontrolörü parametrelerinin ayarlanması için yeni strateji olarak büyük patlama-büyük çöküş optimizasyonu (BBBC) seçilmiştir. İlk olarak, kontrolörler ve yöntem, simülasyon için seçilen paralel hibrit araç aktarma organlarına entegre edilmiştir. Daha sonra, F-PID ve konvansiyonel-PID parametreleri, yakıt tüketimi dikkate alınarak hız referansı ile araç gerçek hızı arasındaki minimum hatayı bulmak için BBBC tarafından ayarlanır. Sonuçlar, Bulanık PID kontrolünün, geleneksel PID kontrol yapısından daha düşük bir yakıt oranına [L / 100km] sahip olduğunu göstermektedir.

Anahtar Kelimeler: Enerji yönetimi, paralel-hibrit elektrikli araç, büyük patlama-büyük çöküş optimizasyonu, bulanık mantık-PID

YILDIZ TEKNİK ÜNİVERSİTESİ
FEN BİLİMLERİ ENSTİTÜSÜ

1
Introduction

1.1 Literature Review

Recently, due to restricted global emission regulations, Hybrid Electric Vehicles (HEV) and Battery Electric Vehicles (BEV) are being more popular. Besides, the vehicles are also encouraged by many governments to reduce air pollution and carbon emission, so that many countries will have pure electric or hybrid electric vehicle in the following years [1].

It is observed that there are many studies, researches, discussions that investigate energy management on Hybrid Electric Vehicles (HEV). While performing energy management between two main power sources, battery and ICE, selected control strategy is subject to optimizing fuel consumption and emission as well as powertrain efficiency. Energy management in hybrid electric vehicles is quite challenging due to vehicle complexity and required data acquisition on torque and speed profiles. In the literature review, existing studies are summarized and are classified as relevant groups. Therefore, control strategies are divided into two groups: Rule-Based control and Optimization-Based control [3].

1.1.1 Rule-Based Energy Management Strategy

Rule based type utilizes human skill and heuristic knowledge of system. Rule-based strategy can be split into two parts which are Fuzzy Control and State Machine Control (SMC) [2]. SMC is related to defining operating mode transition based on battery constraints and driving conditions [3]. Those modes are usually named as charging mode, electric mode, engine mode, hybrid mode and regenerative breaking mode.

In fuzzy control strategy, conventional fuzzy controller application is utilized such as fuzzification, fuzzy rule table, and defuzzification. Fuzzy rule based control types define predetermined linguistic knowledge of application. Methods can be improved to acquire adaptive or predictive solutions. Fuzzy controller can be set by load leveling which utilizes knowledge on driving condition such as road type and driving situation [2]. In addition, another research is about a sophisticated fuzzy controller which contains driver's intention predictor (DIP) and power balance controller (PBC) [4].

One of fuzzy rule based controllers for energy management is identifying a quantity defined as battery working state (BWS) [5]. BWS is adjusted according to battery nominal voltage and state of charge (SOC) to prevent from over-discharge of battery. Power split between battery and engine is achieved by a fuzzy controller considering BWS.

Some inputs are also considered to build a fuzzy rule based controller. S. D. Farrall and R. P. Jones constructed fuzzy universe of investigations as gas pedal data and requested armature current while X. He, M. Parten and T. Maxwell process SOC, and engine torque demand [6, 7]. Furthermore, electric motor speed and driver power demand are considered as data inputs to fuzzy controller.

1.1.2 Optimization-Based Energy Management Strategy

In optimization-based control strategy, the most popular technique is to set up a controller to minimize fuel consumption as cost function. The cost function is derived from system equation and requirements and may be evaluated in terms of fuel consumption, emission, battery ageing, power split depending on powertrain configuration [3]. Basically, the function consists of fuel consumption equation which is subject to physical boundaries of the HEV's powertrain elements like battery current limits, engine torque limits, etc.

Optimization-based strategy is split into three main sub-clusters based on application style. In general, those are called as offline control, real-time control (prediction-based control) and learning-based control strategy. Off-line methods are mainly supposed to gather entire cycle for global optimization. Real-time control strategies account predicted following driving horizon. Learning based method is a kind of machine learning application [8].

One of offline control strategies is Dynamic Programming (DP) method which is very often issued as energy management method is used for determining optimal solutions globally by knowing entire drive cycle and its basic benefit is that it can lightly struggle with system boundaries and non-linearity of system equations [9]. In addition to that, some applications support identifying rule-based strategies [10]. C. Lin, H. Pengl, and J.W. Grizzle tried to gather stochastic modeling of driver request to fix optimization problem via stochastic dynamic programming [11].

Genetic Algorithm (GA) method as off-line control is also studied for energy management in HEVs. In the strategy, power optimization is done depending on engine status to find relationship between e-motor current and engine fuel consumption and Quadratic Programming (QP) is used for gathering optimal battery power based on engine power limits [12]. Another release as GA application is utilized by Fuzzy-PID controller type for vehicle velocity control on HEVs is usually studied for power split powertrain structure [13]. To the my best of knowledge, There is a lack of study in the literature that applies Fuzzy-PID controller in the other powertrain type.

The main aspect of real time control method in HEVs is that solving optimization problem with predicted torque demand and driving road map [9]. MPC and ECMS / PMP is assigned as real time control strategy classification.

The ECMS application which is the most popular strategy is used with Pontryagin's Minimum Principle to find optimized fuel consumption cost function [14]. Hamiltonian function is defined in the ECMS to manage the balance between fuel consumption and various costs in the system such as battery discharge power, battery ageing, etc. Adaptive ECMS (A-ECMS) aims adapting equivalence factor according to changing environment conditions. B. Gu and G. Rizzoni developed ECMS according to driving pattern recognition to release an adaptive algorithm for HEV energy management [15].

For learning based control strategy, two types are reviewed in literature. One of these control strategies is called as Q-learning algorithm. In [16], it is developed with Neuro-Dynamic Programming (NDP) including predicted future road map information which is able to obtain in-vehicle learning. The other learning-based method is defined as Reinforcement Learning (RL). In [17], management works like that system captures rest of trip map via Global Positioning System (GPS) and the algorithm tries to learn adjusted future energy behavior.

1.1.3 Strategy Summary

As a result of these literature survey activities, HEV energy management strategies are classified and illustrated as a structural column in Figure 1.1.

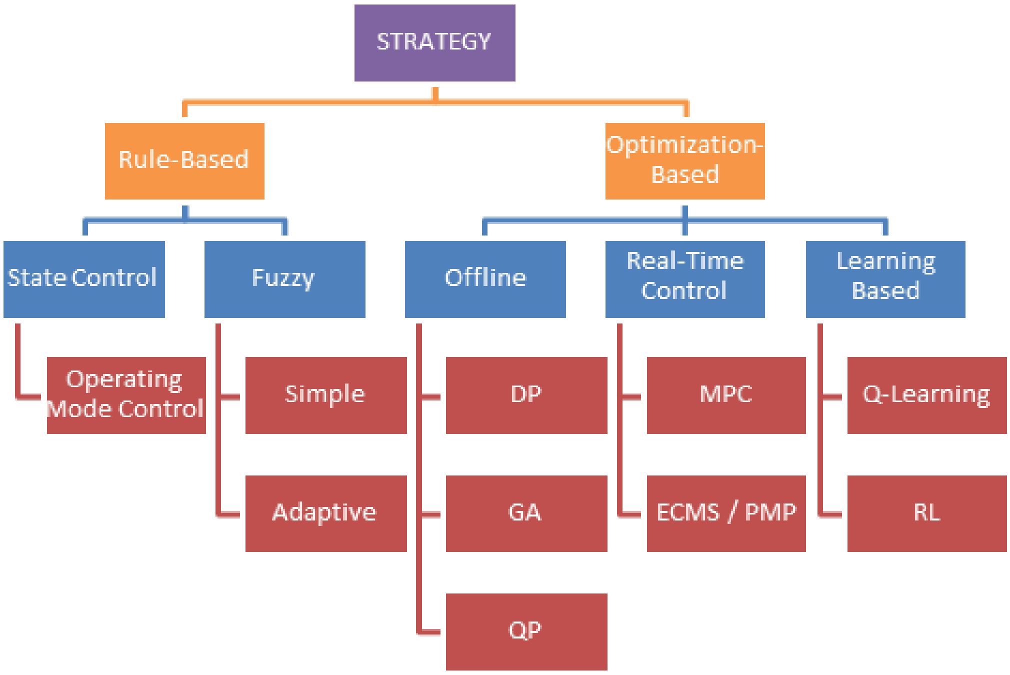

Figure 1.1 Control Strategy Structure in Literature

1.2 Objective of the Thesis

There are many studies that issue optimization of energy management and fuel consumption of HEVs. Main objective of the thesis is to apply a new optimization method to decrease fuel consumption and CO_2 emission in HEVs which have parallel type powertrain structure. In addition, it is also examined that the difference between conventional PID and Fuzzy-PID vehicle control in terms of fuel consumption.

1.3 Hypothesis

The novelty of thesis is that Fuzzy-PID controller combined to big bang-big crunch optimization method is implemented to energy management without battery SOC control. Moreover, that kind of application has never been employed in power and energy optimization of parallel-HEVs. In addition, there is lack of resource about Fuzzy-PID controlled parallel-hybrid electric vehicle topology for energy management.

2
Vehicle Model

HEVs have two propulsion sources as ICE (Internal Combustion Engine) and battery. Energy management plays a critical role in determining power split between those power sources by considering system constraints. Therefore, energy management system (EMS) in HEVs is quite challenging and complicated due to many variances like driver demand, route condition, High Voltage battery capability, vehicle range, CO_2 emission, etc.

2.1 Basic Hybrid Powertrain Topologies

Basically, HEVs are classified in 3 main powertrain configurations which are titled as Series, Parallel and Series-Parallel (Power Split) [18]. In series topology, HV Battery is basic energy source for traction, ICE (Internal Combustion Engine) is used for charging the battery in order to extend vehicle range. Series HEV style is shown in Figure 2.1.

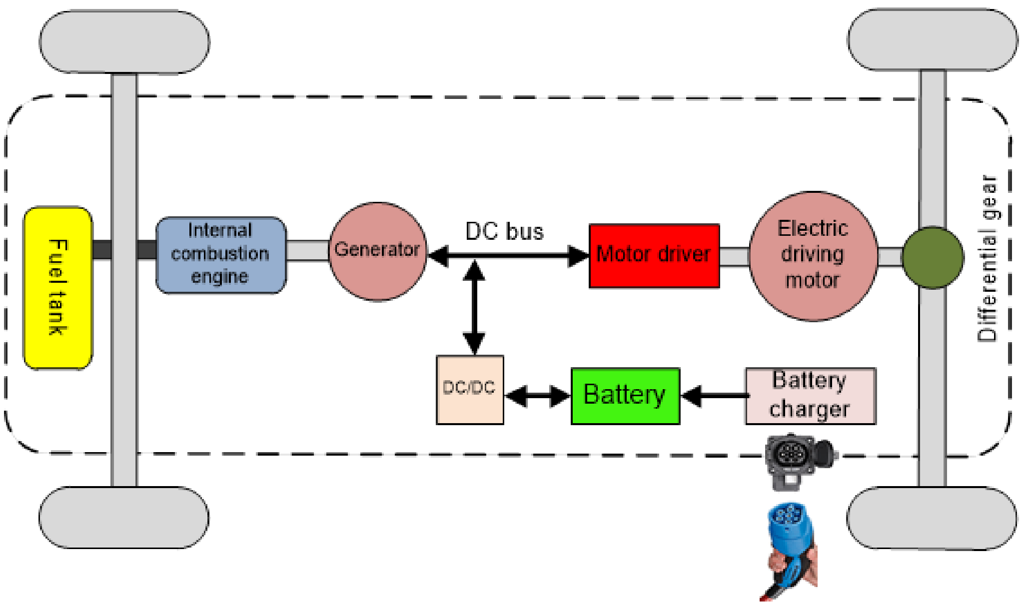

Figure 2.1 Series HEV Topology [19]

In parallel topology, HV Battery and ICE are basic energy source for traction. Both energy sources are used for power demand separately or in combination [14]. Parallel HEV style is illustrated in Figure 2.2. Hybrid topology to be utilized in the study is Parallel HEV model. Parallel HEV powertrain equation will be obtained via relevant vehicle model to be selected.

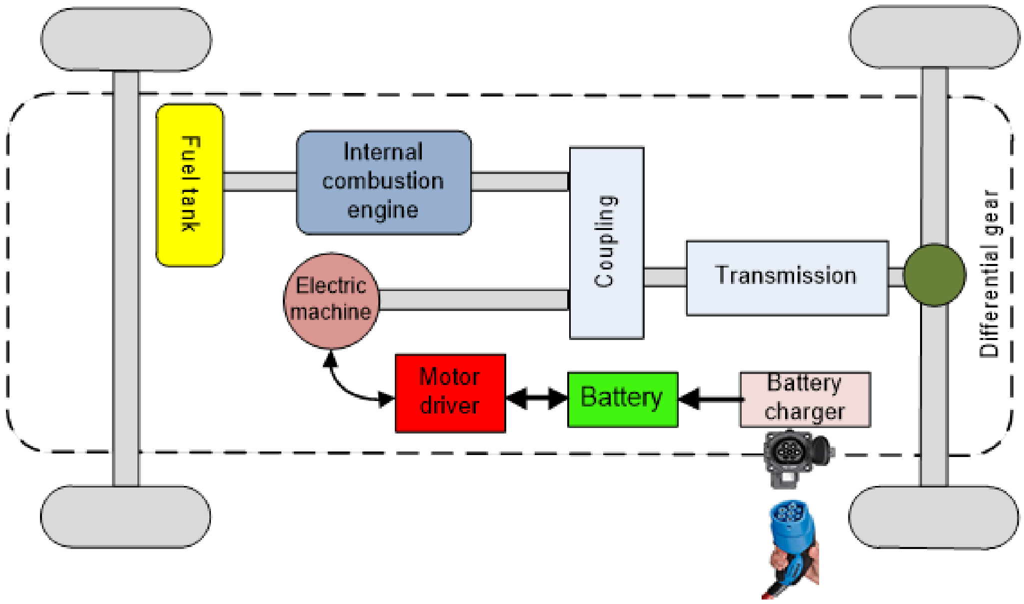

Figure 2.2 Parallel HEV Topology [19]

In power split topology, both series and parallel energy sources are combined to each other via planetary gear set. Energy transition strategy is based on many conditions such as power demand by driver, SoC value for battery, etc. Power Split HEV style can be seen in Figure 2.3.

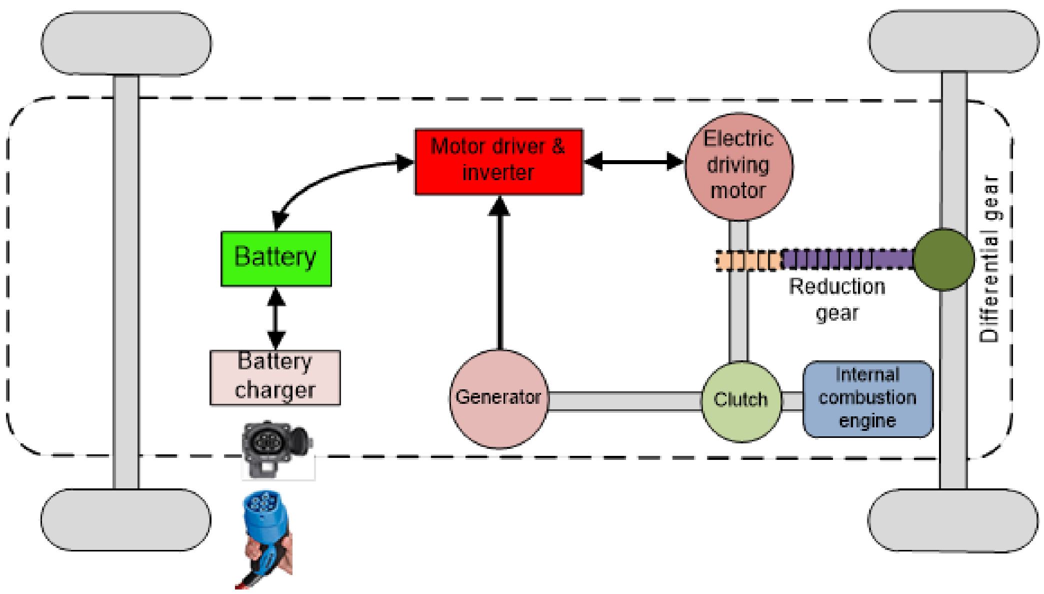

Figure 2.3 Power Split HEV Topology [19]

2.2 Vehicle Longitudinal Dynamics

Equation of vehicle longitudinal dynamics (2.1) is obtained from Newton's second law of motion and vehicle diagram with related forces can be found in Figure 2.4.

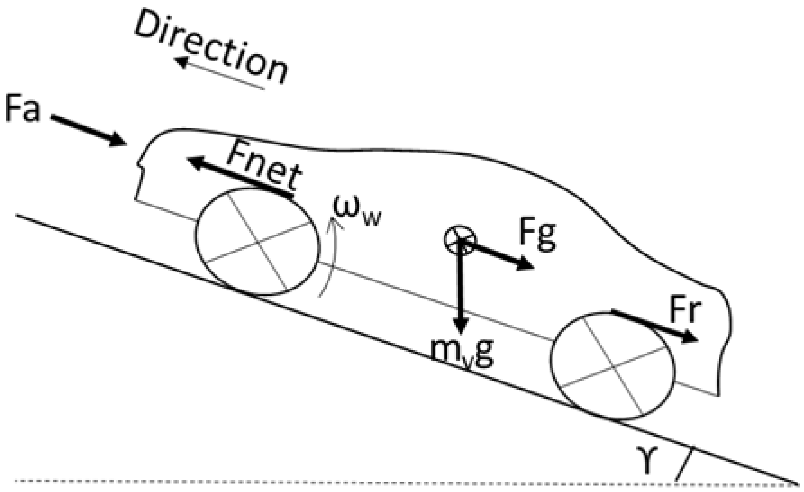

Figure 2.4 Vehicle Traction and Resistance Forces

$$F_{net} - F_a - F_r - F_g - J_{pt}\dot{\omega}_w = m_v a_v \tag{2.1}$$

$$F_a = \frac{1}{2}\rho_{air} c_d A v^2(t) \tag{2.2}$$

$$F_r = c_r m_v g \cos\gamma \tag{2.3}$$

$$F_g = m_v g \sin\gamma \tag{2.4}$$

The formulas are derived to;

$$\frac{d\vartheta(t)}{dt} = \frac{1}{m(t)}\left(\frac{T_{net}}{r_w} - \frac{1}{2}\rho_{air} c_d A v^2(t) - c_r m_v g \cos\gamma - m_v g \sin\gamma\right) \tag{2.5}$$

m(t) parameter given in (2.5) is calculated as;

$$m(t) = m_v + \frac{J_w}{r_w^2} + \frac{J_m n_g^2(t)}{r_w^2} \tag{2.6}$$

where F_{net} is total traction force; F_a is aerodynamic drag force; F_r wheel rolling resistance force; F_g is gravitational force due to road slope; J_{pt} is equivalent inertia of vehicle; ω_w is wheel rotational speed; m_v is vehicle mass; a_v is vehicle acceleration; ρ_{air} is air density; c_d drag coefficient; A is vehicle frontal area; is vehicle velocity; c_r rolling resistance coefficient; g is gravitational acceleration; T_{net} is total net torque; r_w is wheel radius; J_w is total inertia of wheels; J_m is e-motor inertia; n_g is gear ratio [20].

Vehicle and powertrain elements' specification related to a passenger car which has been applied to simulation are demonstrated in Table 2.1.

Table 2.1 System parameters used in simulation

System	Parameter	Value [Unit]
Vehicle	Mass	1200 kg
	Frontal Area	2.46 m^2
	Wheel Radius	0.32 m
	Wheels' Total Inertia	3.78 kgm^2
	Air Density	1.24 kg/m^3
	Rolling Res. Coefficient	0.012
	Air Drag Coefficient	0.25
	Gravity	9.81 m/s^2
	Brake Actuator Bore Diameter	50 mm
	Mean Radius of Brake Pad	150 mm
	Brake Pressure	1 MPa
	Number of Brake Pads on Each Wheel	2
Electric Motor	Inertia	0.00435 kgm^2
	Max Torque	120 Nm
	Min Torque (Generator Mode)	-120 Nm
	Max Speed	6000 rpm
	Power	20 kW
	Efficiency	90%
Engine	Max Torque	155 Nm
	Max Speed	5000 rpm
	Power	90 kW
Battery	Capacity	40 Ah
	Installed Energy	10.36 kWh
	Min Voltage	201.6 V
	Max Voltage	303.8 V
	Current Limits (Charge/Discharge)	-80 A / 80 A
	Continuous Power (Charge/Discharge)	-10 kW / 10 kW
	Max. Power (Charge/Discharge)	-20.7 kW / 20.7 kW
	Number of cells in series	72
	Number of cells in parallel	1

Overall vehicle Simulink model is given in Figure 2.5. Vehicle representative model consists of three main blocks which are 'Driver Demand', 'Hybrid Control System', 'Powertrain'. Driver Demand block where controller is placed creates requested torque based on speed reference and actual vehicle speed. According to driver demanded torque, Hybrid Control System block decides traction torque split between engine and motor. In case braking, it defines required regenerative braking and frictional braking torques and the block sends the torque value to powertrain block. In addition to torque data, it also provides gear number decided on AP position and vehicle velocity.

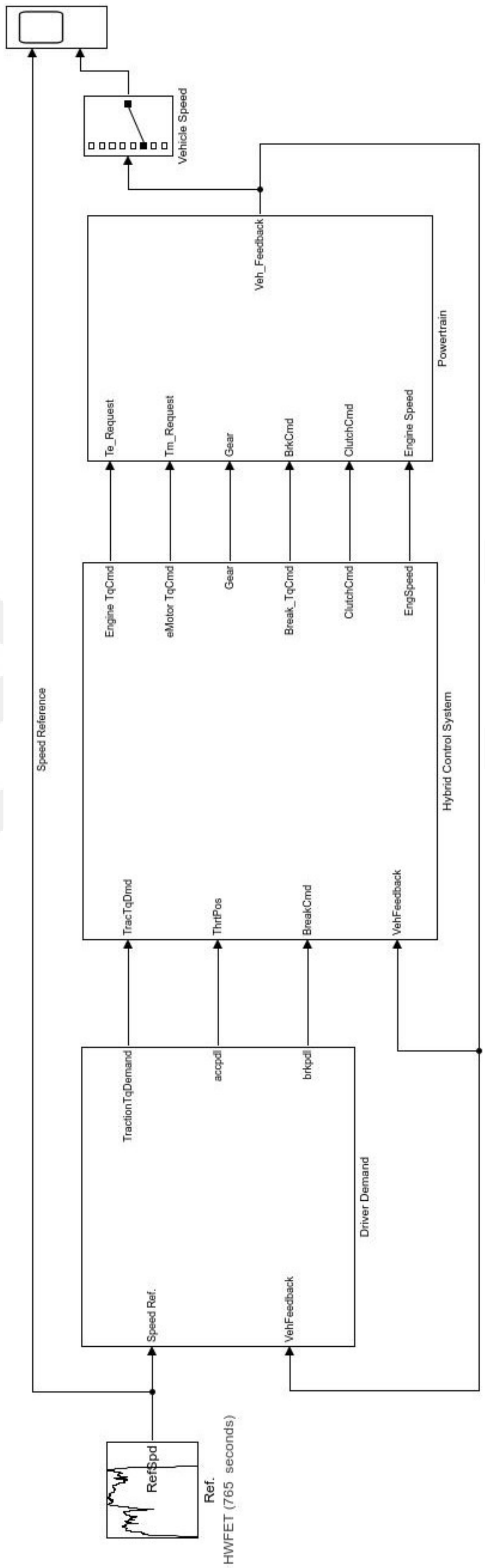

Figure 2.5 Vehicle System View in Simulink

2.3 Driver Demand Model

Driver Demand block contains controller structure and it releases required torque for traction or brake. Traction torque request is equal to product of by multiplying acceleration pedal (AP) position rate and instant total torque capability of engine and motor and it is given in (2.9). Brake pedal (BP) position rate is sent to hybrid control system for braking block. Acceleration and brake pedal position rates are also illustrated in (2.7) and (2.8) and they are depended control input of controller block. Torque demand, AP and BP are obtained like;

$$\varphi_A(t) = \begin{cases} 1 & \text{if } u(t) > 1 \\ u(t) & \text{if } 1 \geq u(t) \geq 0 \\ 0 & \text{if } u(t) < 0 \end{cases} \tag{2.7}$$

$$\varphi_B(t) = \begin{cases} 0 & \text{if } u(t) > 0 \\ u(t) & \text{if } -1 \leq u(t) \leq 0 \\ -1 & \text{if } u(t) < -1 \end{cases} \tag{2.8}$$

$$T_d(t) = T_s(t)\,\varphi_A(t) \tag{2.9}$$

where φ_A is acceleration pedal position rate; φ_B is brake pedal position rate, u is control input; T_s is instant traction torque capability of vehicle system; T_d is torque demand sent to traction block in hybrid control system.

As an example, Fuzzy-PID driver demand model can be found in Figure 2.6.

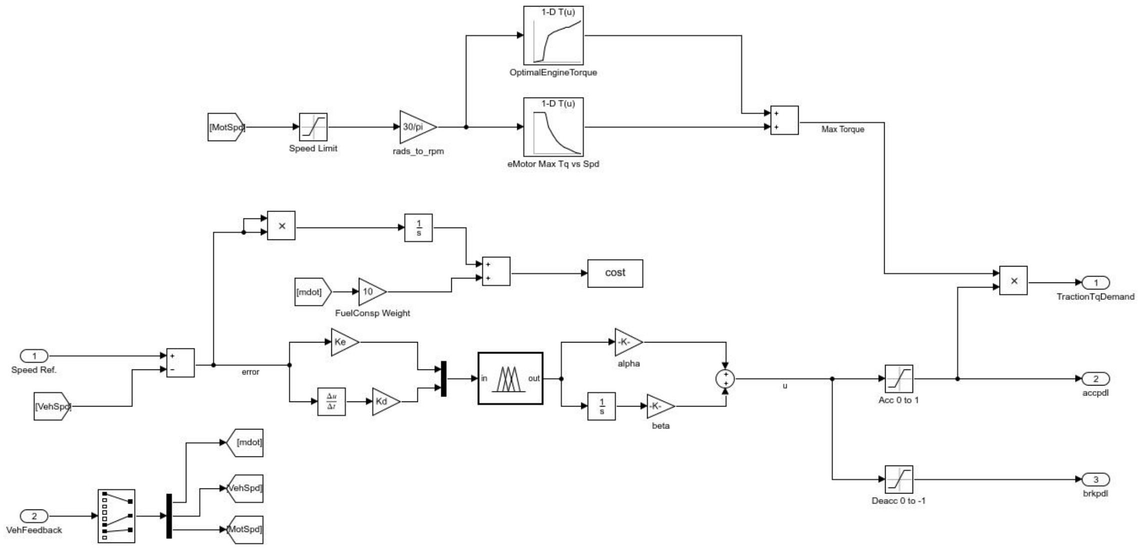

Figure 2.6 Driver Demand Block

2.4 Hybrid Control System Model

Hybrid control system is constructed as it contains traction model, brake model and gear selection model. The model processes following inputs: traction torque command, AP and BP positions, feedback from powertrain system such as battery SOC, motor speed, etc. Then, it releases required traction torque split between motor and engine, brake torque, clutch command, gear number. Model representative overview is given in Figure 2.7.

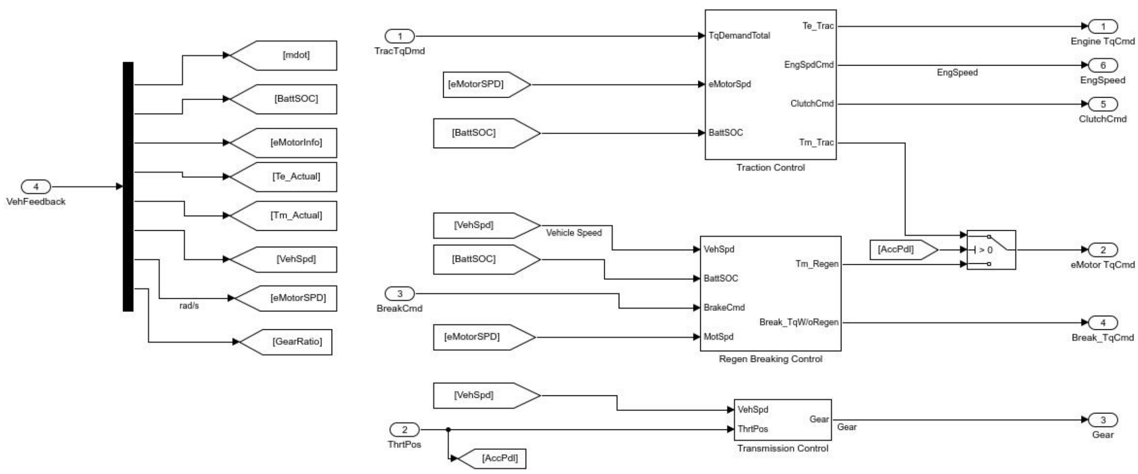

Figure 2.7 Hybrid Control System Block Overview

2.4.1 Traction Model

According to torque demand, if AP position is greater than zero, traction, generates related toque for engine and motor within their limits. Firstly, model checks if requested torque is covered by motor and it is in battery discharge limit. As long as motor and battery satisfy the demand, engine is in off status and clutch is in dis-engaged mode. This is also called as ‘Electric Drive’. Block overview is demonstrated in Figure 2.8. Motor is always initial traction element in the powertrain. That means mobility starts at electric drive mode.

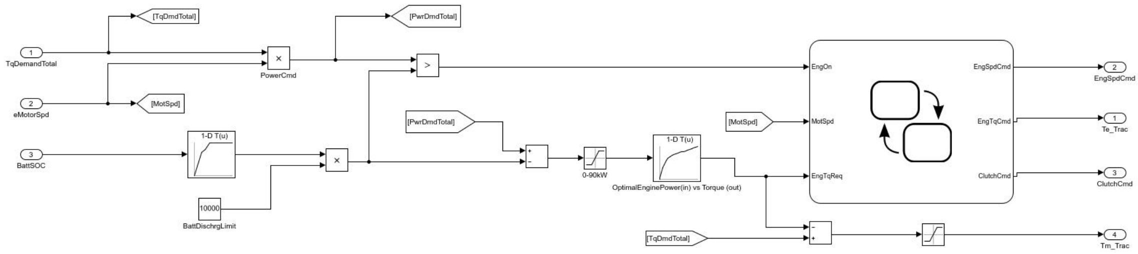

Figure 2.8 Traction System Block Overview

Transition between hybrid mode (traction by both engine and motor) and electric drive mode, it is handled by state flow diagram in the model as it requires engine on-off control, engine idling status, clutch on-off control, etc. Engine control strategy starts to work once Engine ON signal is triggered if requested torque is not handled by motor. Engine status is decided to follow like flowchart in Figure 2.9.

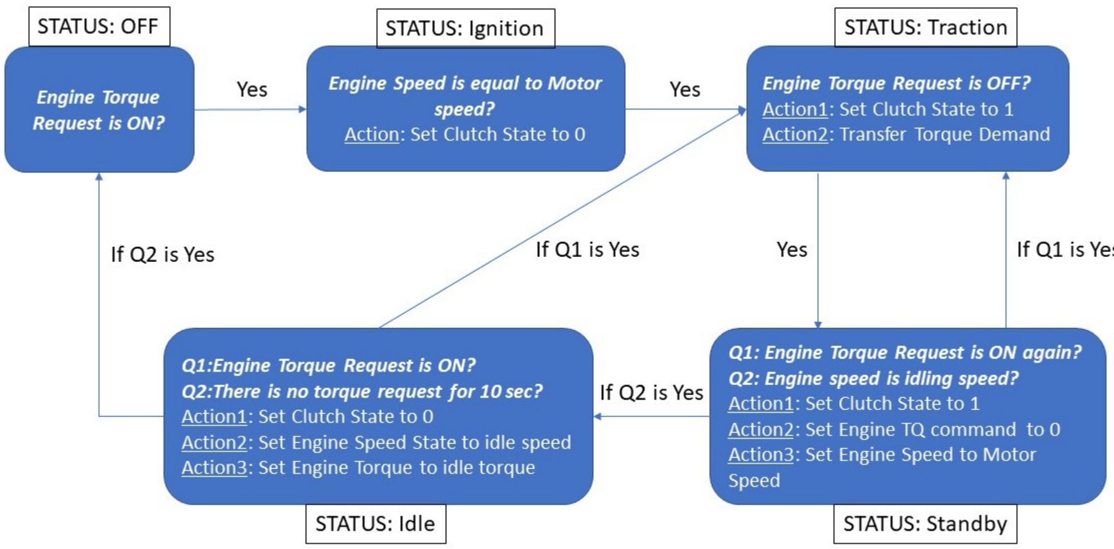

Figure 2.9 Engine System Integration Flowchart

2.4.2 Vehicle Brake Model

Parallel brake type including both frictional braking and regenerative braking is applied, brake parameters come from MATLAB brake disc model block. Frictional brake equation shown in (2.10) is formulated as;

$$T_b(t) = N_{brake} \frac{\mu_k \pi {D_b}^2 R_m N_{pads} P}{4} \varphi_B(t) \tag{2.10}$$

where T_b is brake torque on wheels; N_{brake} is number of brakes, μ_k is disc pad-rotor coefficient of kinetic friction; D_b is brake actuator bore diameter, R_m is mean radius of brake pad force application on brake rotor which is equal to average radius of brake pad to the hub; N_{pads} is number of brake pads on each wheel, P is applied brake pressure.; φ_B brake pedal position rate [21].

Regenerative brake torque is based on that instantaneous negative motor torque as generator mode and it is proportional of both brake pedal position rate and regen factor depended on vehicle speed and battery charge limits. Speed related factor works like that it assigns proportional coefficient between 0 and 1 according to between 0-9 km/h. If velocity is greater than 9 km/h, the factor is equal to 1. On the other hand, battery charge limit factor value is that it is proportional constant between 0 and 1 according to battery SOC due to battery characteristic. If battery SOC is lower than 70%, the factor is 1. In case battery SOC is higher than 70%, then factor decreases to 0 proportionally and it is assigned to 0 when battery is fully charged. Vehicle Brake model is seen in Figure 2.10.

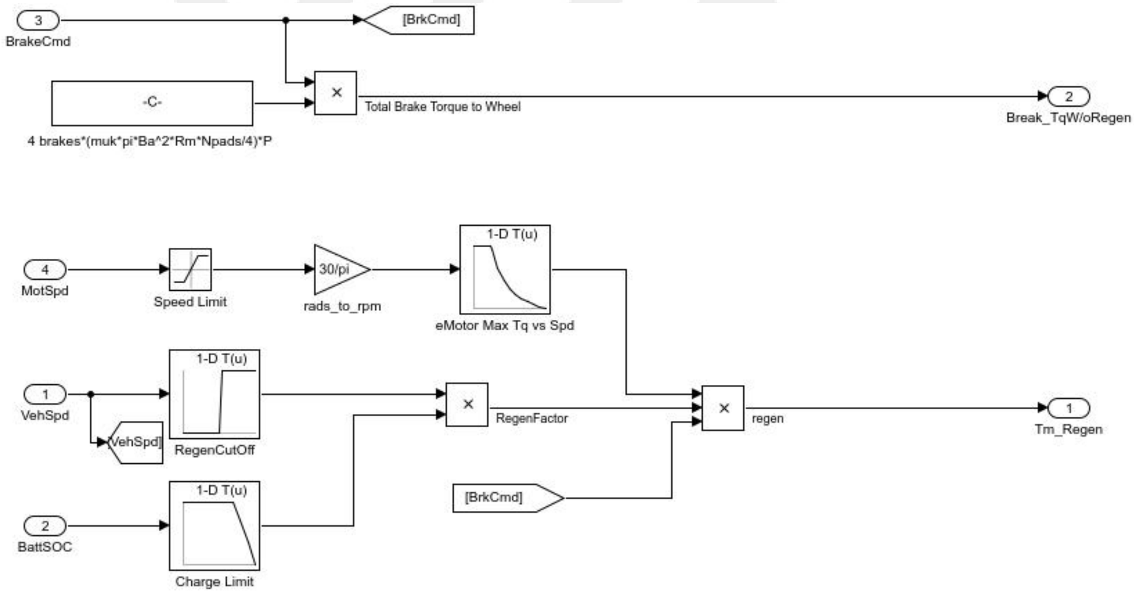

Figure 2.10 Brake Model Block in Simulink

2.4.3 Gear Selection Model

Gear up-shift / down-shift decision map based on throttle position and vehicle speed is shown in Figure 2.11. During acceleration, up-shift lines are reference points and while vehicle is decelerating, dotted downshift lines are considered in the system model. Gear number decision is made via state flow block of Simulink tool. Lines refer to shifting threshold. For example, if we consider initial condition that acceleration pedal is pressed to 50% constantly, vehicle speed is 0 km/h and gear is 1, gear will be shifted to 2 when vehicle speed is higher than 30 km/h.

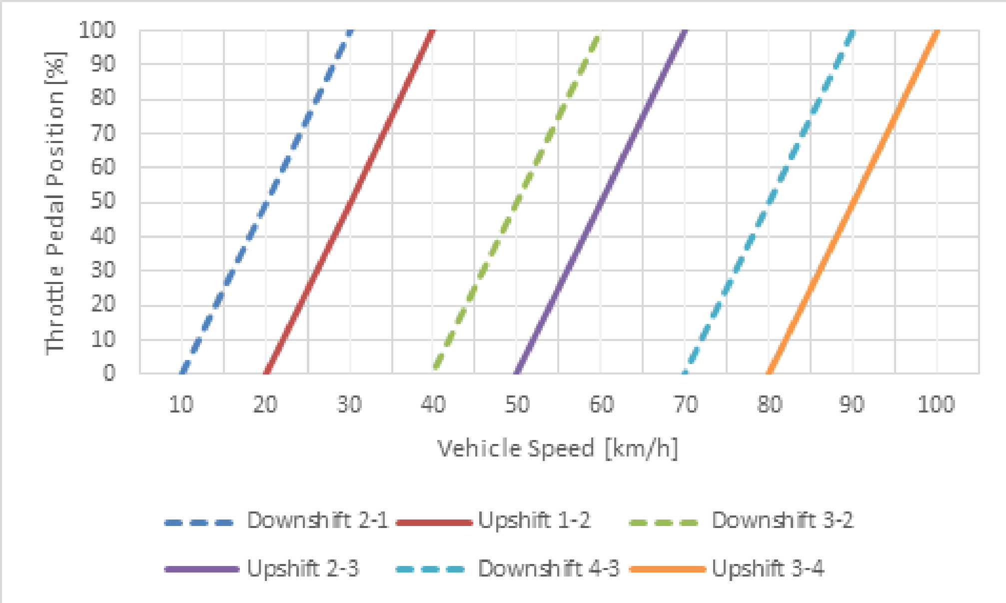

Figure 2.11 Transmission System Gear Selection Map

2.5 Powertrain Model

Parallel hybrid powertrain has following elements: battery, motor, engine and transmission system and detailed representative model is touched in the following chapters. Signal output of the block which is called as vehicle feedback is utilized by driver demand block and hybrid control system. Vehicle feedback signal includes fuel flow rate, battery SOC, motor speed, vehicle speed, actual engine, motor torque and gear ratio. System drivetrain is illustrated in Figure 2.12 and it is transferred to Simulink block like given in Figure 2.13.

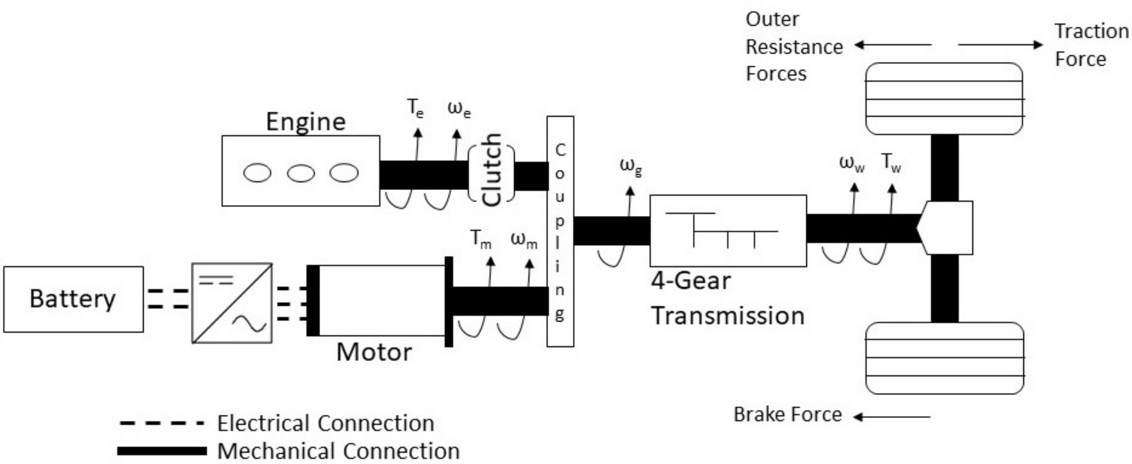

Figure 2.12 Powertrain Demonstration

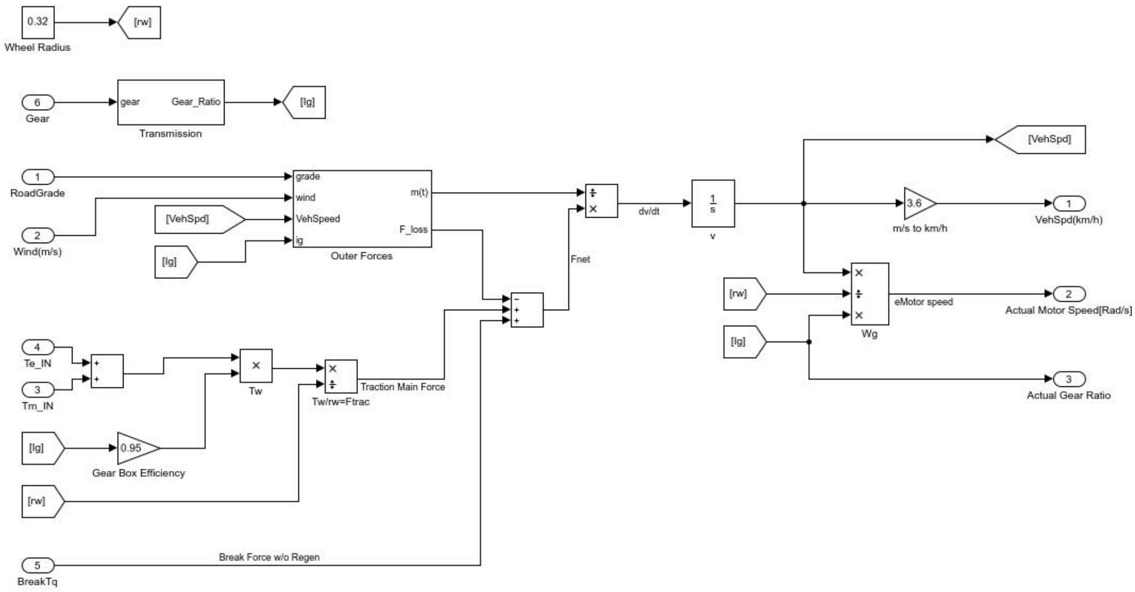

Figure 2.13 Drivetrain Block Overview

Model in Figure 2.13 and demonstration model in Figure 2.12 are based on formulas given in Chapter 2.2.

2.5.1 Electric Motor Model

Electric motor model is based on a map in Simulink model instead of creating its dynamic equations. It is presumed that efficiency between mechanical power and electrical power is constant as 90% at every operating condition of motor and the model works as if it delivers required torque within constraints indicated as;

$$0 \leq \omega_m(t) \leq \omega_{m,max} \tag{2.11}$$

$$T_{m,min} \leq T_m(t) \leq T_{m,max} \tag{2.12}$$

where ω_m is motor rotational speed; T_m is motor torque and min torque value refers to the highest torque during generator mode. Therefore, motor is assumed that it is capable to provide relevant performance during energy generating.

Torque and speed of motor map is given in Figure 2.14.

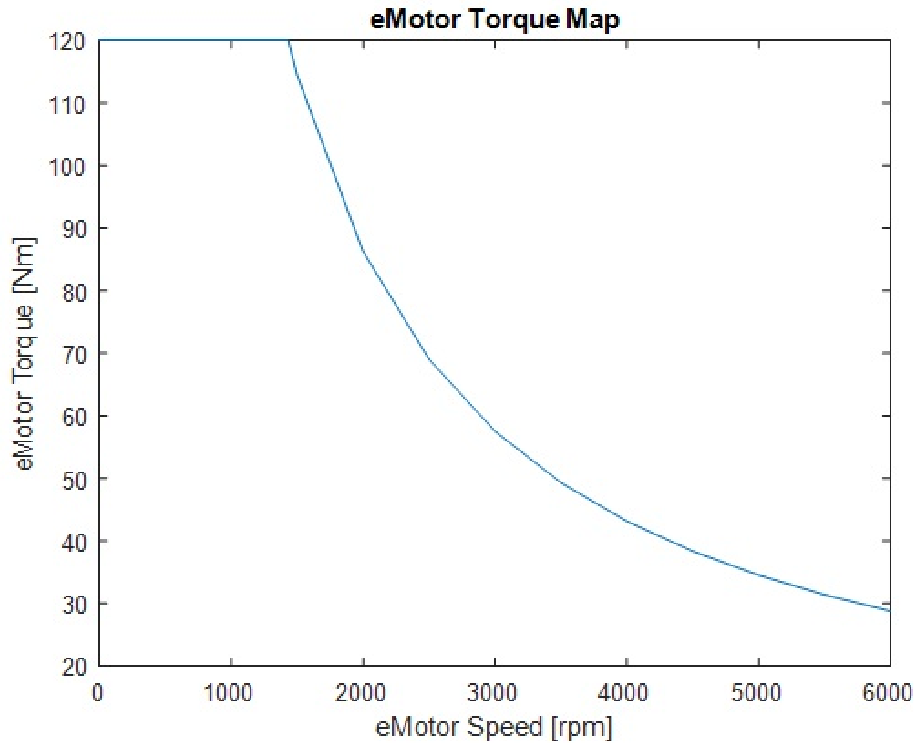

Figure 2.14 Motor Torque vs Speed Map

Detailed information about motor model can be seen in Figure 2.15. Equation (2.13) is carried over from mapped motor model in MATLAB Simulink tool and it is set up in motor model. Motor power formula is expressed as;

$$P_m(t) = \omega_m(t)\, T_m(t) \tag{2.13}$$

where P_m is mechanical output power of motor.

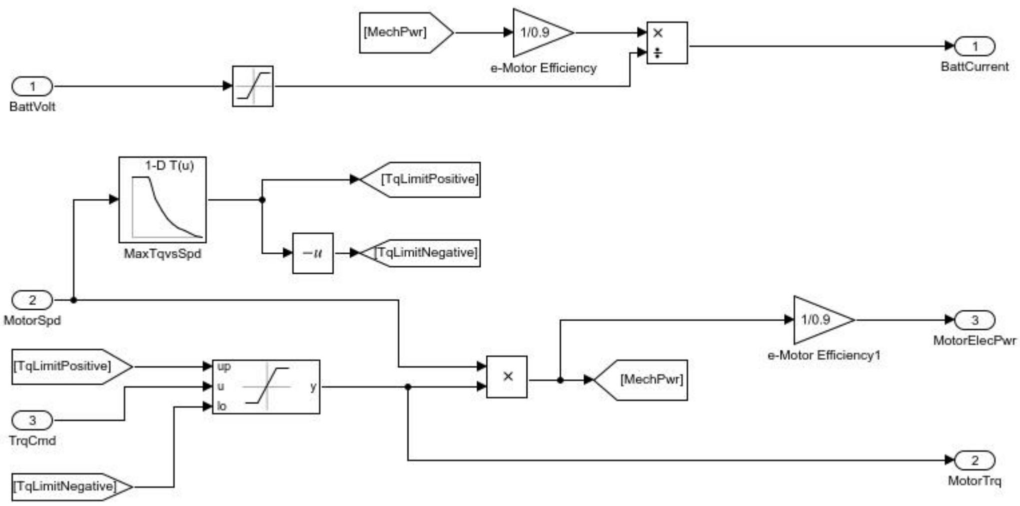

Figure 2.15 Motor Block Overview in Simulink

2.5.2 Engine Model

Engine is modeled as a map in Simulink and it is considered that engine provides torque demand from driver as long as request does not exceed element boundaries which are defined as;

$$0 \leq \ \omega_e(t) \ \leq \ \omega_{e,max} \tag{2.14}$$

$$0 \leq \ T_e(t) \ \leq \ T_{e,max} \tag{2.15}$$

where ω_e is engine rotational speed; T_e is engine torque. Relationship between engine torque and speed is demonstrated in Figure 2.16.

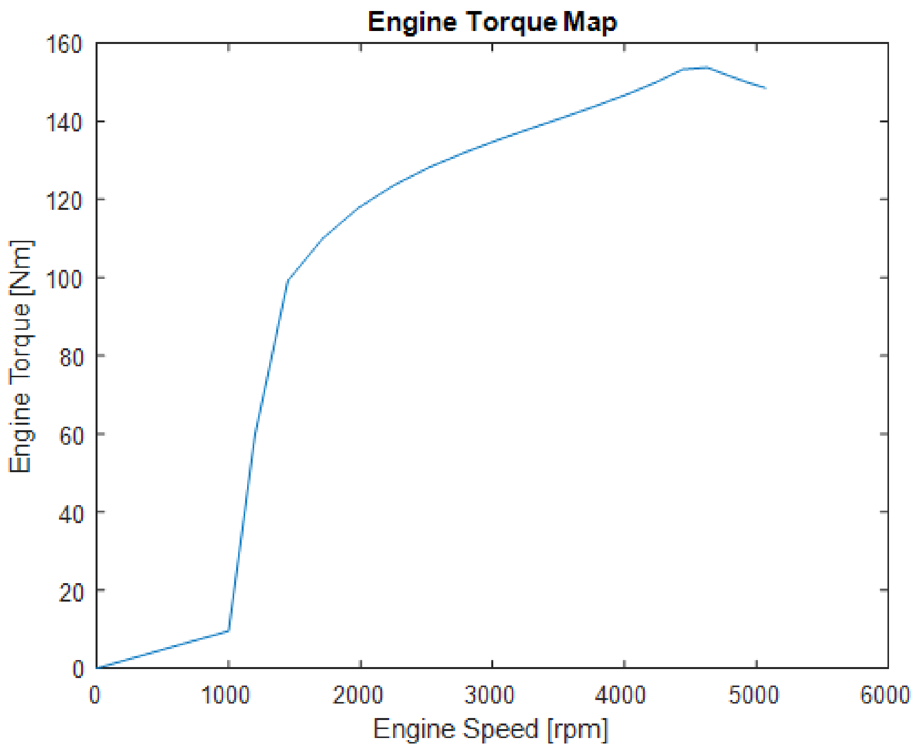

Figure 2.16 Engine Torque vs Speed Map

Fuel consumption and CO_2 emission are function of engine speed and torque and are obtained from a map indicated in Figure 2.17 and Figure 2.18 respectively. Related equations are set up like;

$$\dot{m}_f(t) = f_{fuel}(\omega_e(t), \ T_e(t)) \tag{2.16}$$

$$\dot{m}_{CO2}(t) = f_{emission}(\omega_e(t),\ T_e(t)) \tag{2.17}$$

where $\dot{m}_f$ is mass of fuel consumption; $\dot{m}_{CO2}$ is mass of emitted CO_2.

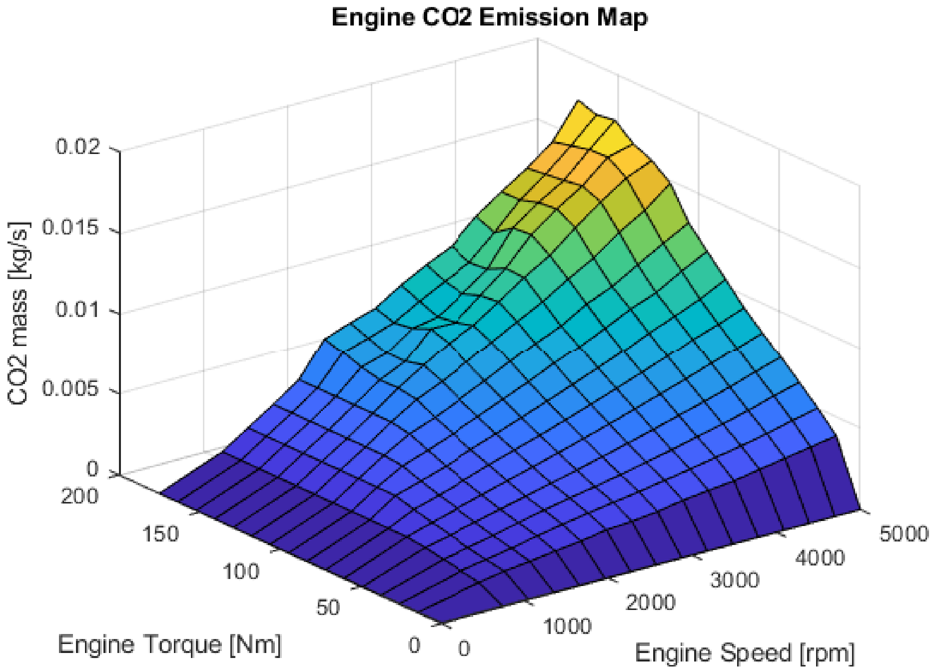

Figure 2.17 Corresponding Engine CO_2 Emission Map Based on Speed and Torque

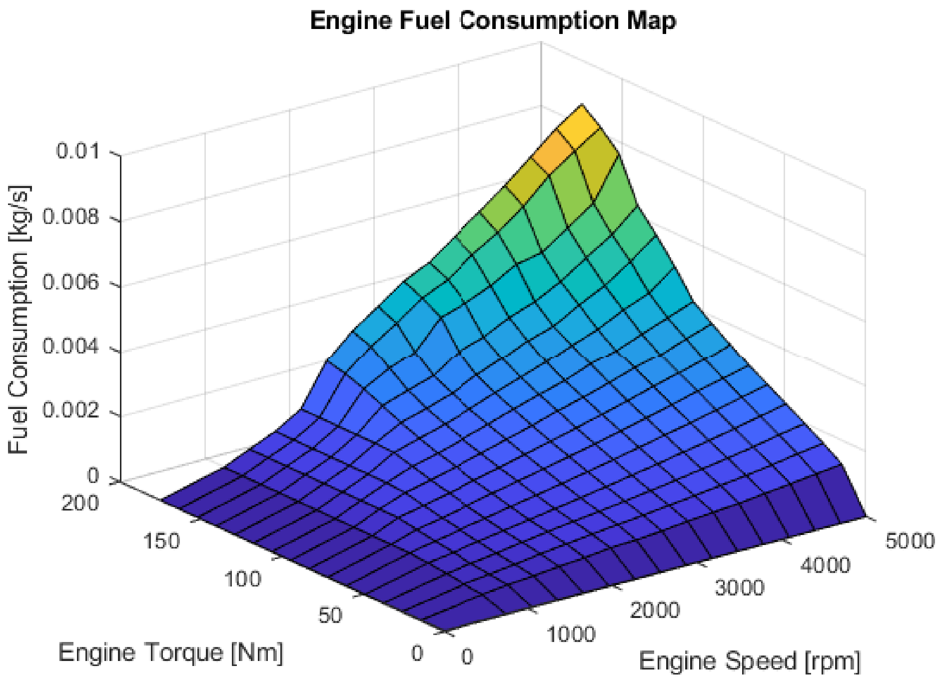

Figure 2.18 Corresponding Engine Fuel Map Based on Speed and Torque

Like issued in motor Simulink model, engine block is also modeled as if it delivers needed torque within engine constraints the model is illustrated in Figure 2.19. Look-up Table feature defined as a map is utilized for engine emission and fuel and all map data is obtained from mapped engine model in MATLAB Simulink tool. In addition, required engine torque is passed if clutch signal is ON which means engaged status. Clutch signal is decided by Hybrid Control Block and traction control subject is touched in chapter 2.4.1.

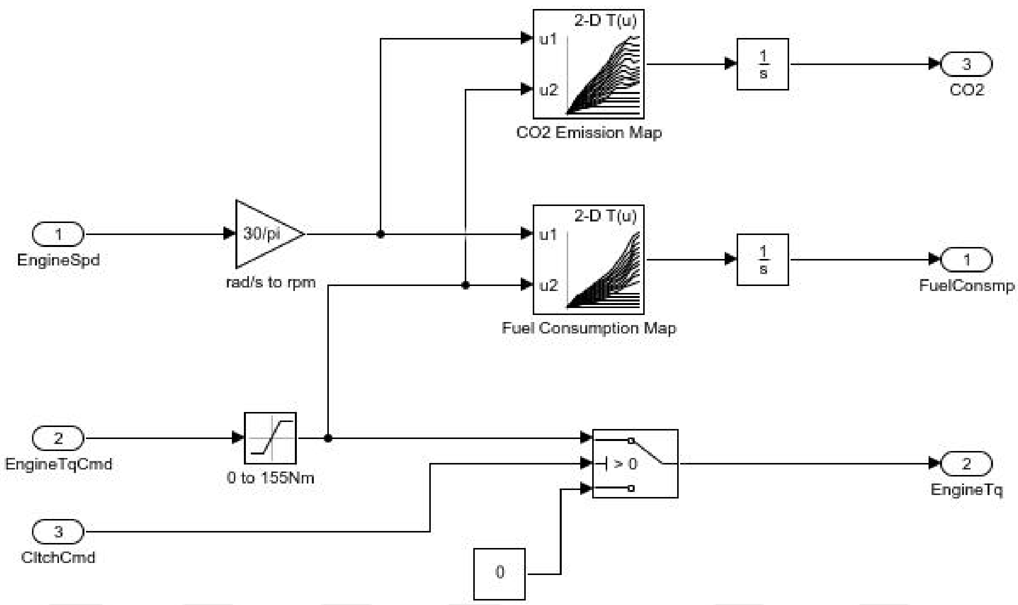

Figure 2.19 Engine Block Overview in Simulink

2.5.3 Battery Model

Lithium – Ion battery is represented by two types of math model which feed HEVs and full electric vehicle studies [22]. Those types are circuit based and electrochemistry based which refers to chemical reaction dynamics in a cell. In the model, basic battery equivalent circuit for a cell representation is considered and it is shown in Figure 2.20. In the circuit, one cell is modeled as if it consists of a voltage source (U_{oc}) which is open circuit voltage (OCV) and serial internal resistance (R_i) depending on temperature.

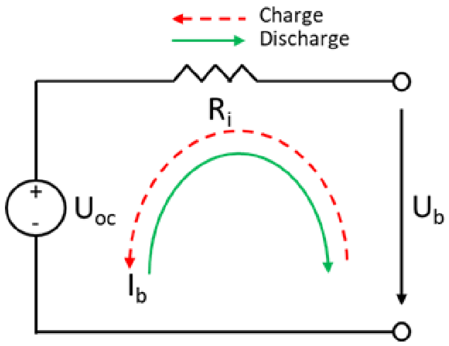

Figure 2.20 Basic Battery Equivalent Circuit [22]

According to basic battery equivalent circuit, following battery level (2.18) and (2.19) electrical equations can be written as;

$$U_b = U_{oc}(t) - I_b(t)R_i(t) \tag{2.18}$$

$$I_b(t) = \frac{U_{oc}(t) - \sqrt{U_{oc}^2(t) - 4R_i(t)P_m(t)}}{2R_i(t)} \tag{2.19}$$

where U_b is cell terminal voltage; U_{oc} is cell open circuit voltage; I_b is battery current; R_i cell internal resistance; P_m is motor power.

A cell OCV for a Li-Ion battery is depended on temperature, state of charge (SOC) and cell chemistry [23]. Applied OCV vs SOC curve at constant battery temperature 25^oC in the vehicle model for simulations is demonstrated in Figure 2.21 which is carried over from MATLAB Simulink battery model. During battery operation, it is assumed that battery temperature is constant as 25^oC.

SOC calculation is based on equation (2.20) in system simulation. In addition, battery constrains are given in equation (2.21) and (2.22) as;

$$SOC(t) = SOC_{in} - \frac{1}{Q}\int I_b(t)\,dt \tag{2.20}$$

$$I_{b,min} \leq I_b(t) \leq I_{b,max} \tag{2.21}$$

$$SOC_{min} \leq SOC(t) \leq SOC_{max} \tag{2.22}$$

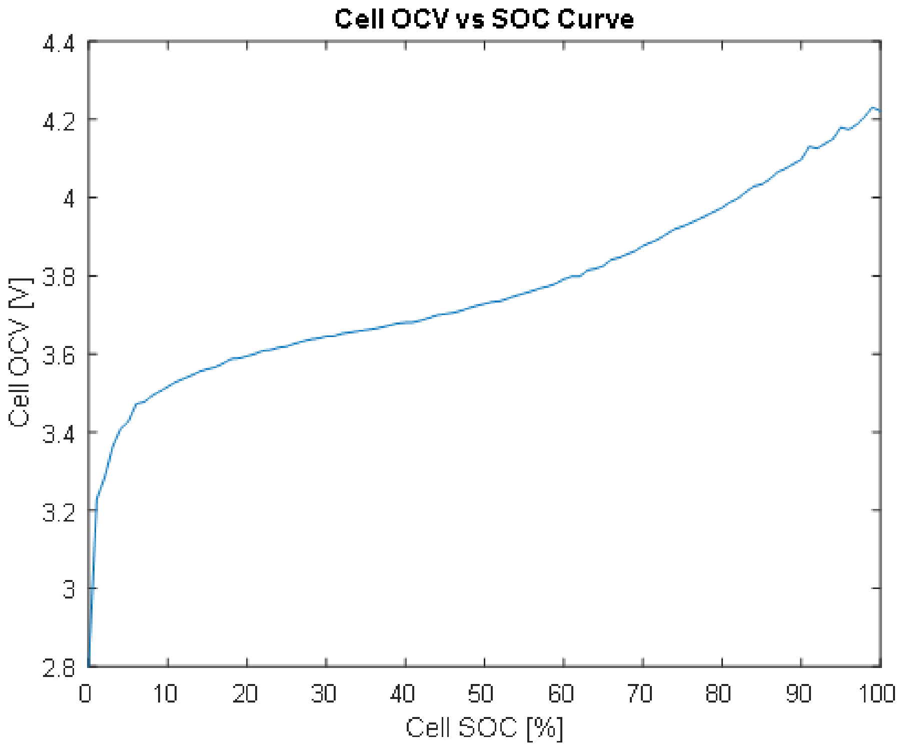

Figure 2.21 SOC vs OCV Curve at $25^{o}C$

where SOC_{in} is initial SOC of battery; Q is battery capacity, I_b is battery current. SOC constraint of battery is not considered in this study as applied drive cycle does not require too much power from battery and battery is not started at very low SOC level. However, due to battery properties, there shall be SOC window for operating in vehicles. Otherwise, operating at either high or low level SOC lead to decreasing battery capacity faster than normal operating life-cycle [24, 25].

Aux-power consumption from the battery is ignored during simulations.

2.5.4 Gearbox Model

Gearbox equations are formulated in (2.23) and (2.24) by considering basic transmission dynamics as;

$$\omega_g = \frac{\vartheta(t)}{r_w} n_g(t) \tag{2.23}$$

$$T_w(t) = T_g(t) n_g(t) \mu_g \tag{2.24}$$

where ω_g is gearbox input shaft speed; is vehicle velocity; r_w is wheel radius; n_g is gear ratio corresponding gear number, μ_g gear box efficiency which is assigned as 95% and speed depended losses are neglected.

Gear ratios for each gear value can be seen in Table 2.2.

Table 2.2 Gear ratio values corresponding to gear number

Gear	Gear Ratio
1	10.78
2	5.88
3	3.75
4	2.61

Final drive of modeled vehicle is assumed that it is consisting of 1:1 gear system with neglected efficiency parameter.

3
Big Bang-Big Crunch Based Fuzzy-PID Controller Design

An optimization method should converge to an optimum point, but the method must also contain different points in the search space that are descending in order to be classified as a global method. In other words, most of the newly created individuals should be around the optimum point, but a small part should be spread to the rest of the space.

3.1 Big Bang-Big Crunch Optimization Method

Big Bang-Big Crunch Optimization algorithm based fuzzy modeling software is a map-based modeling software designed in this thesis and is working in MATLAB tool. In 2005, BBBC as a new optimization method was initiated by Osman K. Erol, Ibrahim Eksin who inspired by the Big Bang and Big Crunch Theory [26]. The logic of this method is the transformation of the convergent solution into a chaotic state consisting of a new set of solutions [26]. The most important feature of BBBC optimization algorithm is low projection time where high convergence rate is present [27]. BBBC optimization algorithm was first used in online adaptation of fuzzy model output parameters [28].

Strategy is kind of GA in terms of identifying primary population randomly as indicated in Appendix-A. The BBBC algorithm generally includes two major phases. Main nature of the optimization is that generation of initial population is done during Big Bang phase which is called as first phase. Then, the Big Crunch phase as second phase is chasing the Big Bang phase. In the second phase, the center of the population mass (X_c) or the most appropriate point is calculated. Calculation of X_c is denoted in equation (3.1) or is determined as the smallest value of cost function and Big Bang point is decided. All big-bang items occur around the point in the big brunch phase. Center of mass is computed as;

$$X_c = \frac{\sum_{i=1}^{N} \frac{1}{J_i} X_i}{\sum_{i=1}^{N} \frac{1}{J_i}} \tag{3.1}$$

where X_c center of mass; X_i is position within n-dimensional search section created; J_i is cost function value of this point; N is the population dimension in Big Bang phase. New candidate solutions around the center of mass are computed in (3.2) by including or subtracting a random number whose value reduces as iterations elapse. This can be indicated as;

$$X^{new} = X_c + \frac{ra(X_{max} - X_{min})}{k} \tag{3.2}$$

where X_c center of mass; r is random number; a is parameter limiting factor of the search space; X_{max} and X_{min} are upper and lower limits; k is iteration step. While the number of iterations is increasing, the number of individuals formed far from the optimum point should decrease.

Applied model of this study utilizes equation (3.3) as cost function and population consists of Fuzzy-PID and conventional PID parameters. Because, target is to meet given velocity reference as much as possible in conjunction with minimum consumed fuel rate. Fuel rate value has a weighted factor because fuel mass rate is more important than speed compatibility. BBBC algorithm related equations for studied system are expressed as;

$$\varepsilon(t) = \vartheta_{ref}(t) - \vartheta_{actual}(t) \tag{3.3}$$

$$J = \int \left(\varepsilon(t)^2 + \sigma m_{fuel}(t)\right) dt \tag{3.4}$$

where ε is controller input error; ϑ_{ref} is speed reference; ϑ_{actual} instant speed of vehicle; m_{fuel} is mass of consumed fuel and is function of engine speed and torque; σ is weighted coefficient of consumed fuel.

BBBC algorithm has process steps in sequence and it is given in Table 3.1 [26].

Table 3.1 BBBC algorithm process steps

Step No.	Remark
1	Create an initial generation of N candidates in random way. Mind the limits of the utilization section
2	Evaluate cost function values of all the candidate solutions
3	Find the center of mass according to Eq. (3.1). The best appropriate individual can be selected as the center of mass instead of applying Eq. (3.3).
4	Compute new candidates next to the center of mass by attaching or removing random number whose value reduces as the iterations progress.
5	Return to Step 2 until finishing requirement is achieved

In the thesis, BBBC optimization strategy is combined to Fuzzy-PID and conventional PID controlled systems to find controllers' parameter. Detailed information about system diagrams including controllers can expressed in following chapters.

3.2 Fuzzy-PID Controller Structure

Fuzzy-PID controller could be categorized into three main types as Direct action, gain scheduling, Hybrid fuzzy PID controllers [29]. Direct action type is also divided into three groups based on number of controller input as single, double, triple. In addition, triple input controller has got two sub-cluster as type-1 and type-2 in terms of fuzzy controller layer. All types' hierarchy is illustrated in Figure 3.1.

In this study, system is controlled by double input type Fuzzy-PID and controller parameters are tuned by BBBC algorithm.

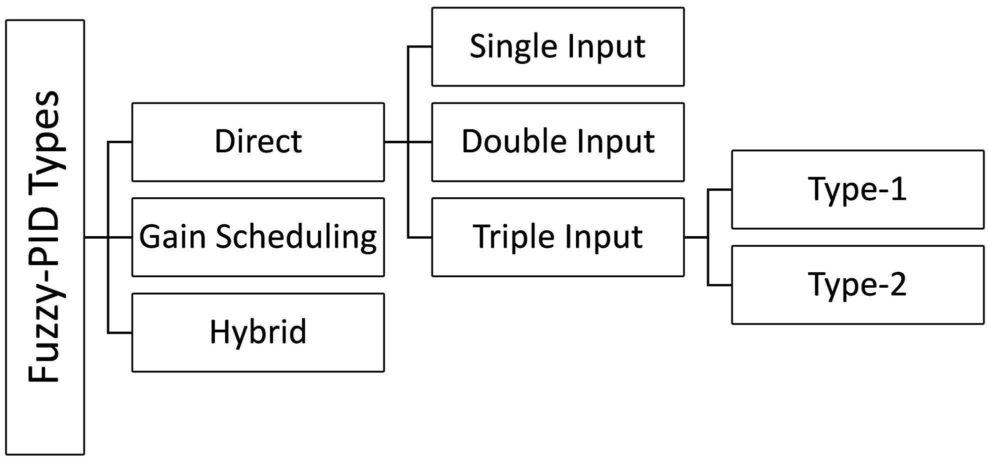

Figure 3.1 Fuzzy-PID Categorization [24]

3.2.1 Direct Action Type Fuzzy-PID Controller

Basic controller of direct type is called as single input. System error is only input for FLC and output is linked to conventional PID structure as seen in Figure 3.2. Therefore, it sets up one dimensional rule.

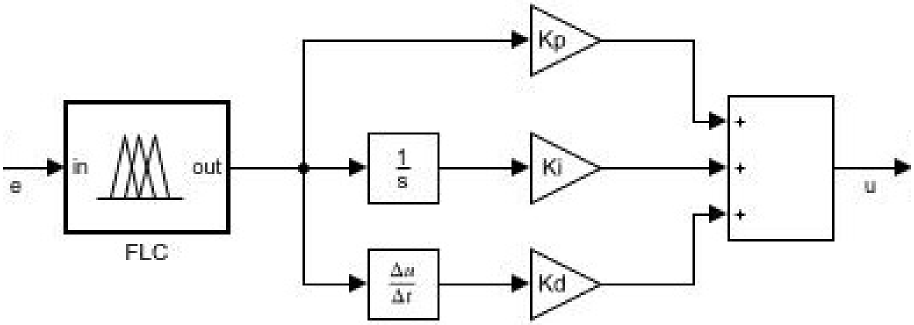

Figure 3.2 Single Input Fuzzy-PID Controller

Second application of direct type is double input which is utilized in system simulations. In this controller type which could be captured by combination of Fuzzy-PI and Fuzzy PD application, inputs are error and its derivative. Figure 3.3 indicates how controller structure is implemented [29].

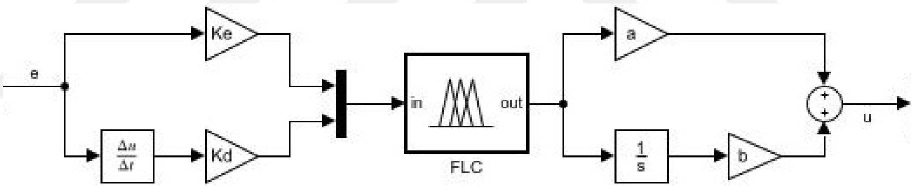

Figure 3.3 Double Input Fuzzy-PID Controller

Triple input controller structure is another member of direct type Fuzzy-PID controller, which contains two types as Type-1 and Type-2. Basically, triple input types include error, error derivative and integral of error. Two types of triple input Fuzzy-PID controller are given in Figure 3.4.

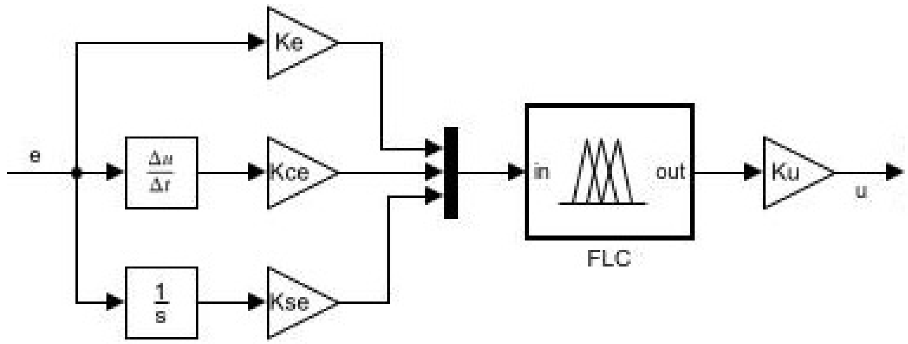

(a)

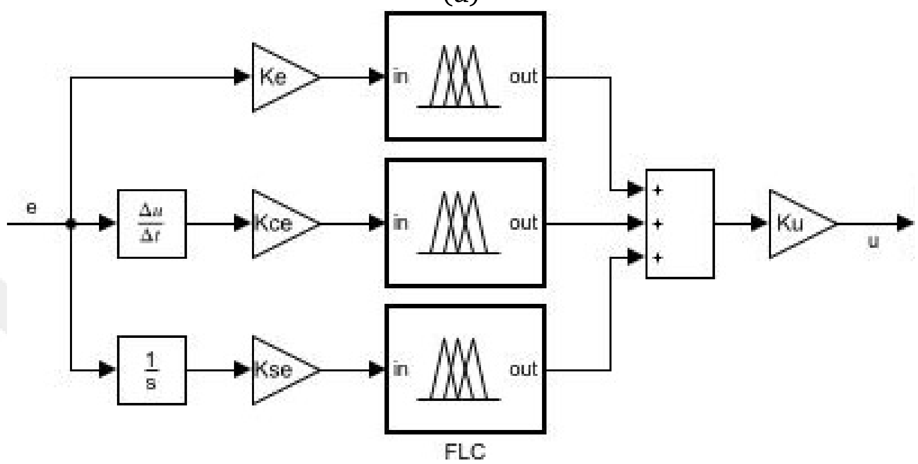

(b)

Figure 3.4 (a)Triple Input Fuzzy-PID Controller Type-1 (b) Type-2

3.2.2 Gain Scheduling Type Fuzzy-PID Controller

This type of Fuzzy-PID controller system contains FLC that determines conventional PID parameters via FLC inference with double input [31]. That kind is used to maintain PID controller as tuned appropriately. Block diagram of the type is illustrated in Figure 3.5.

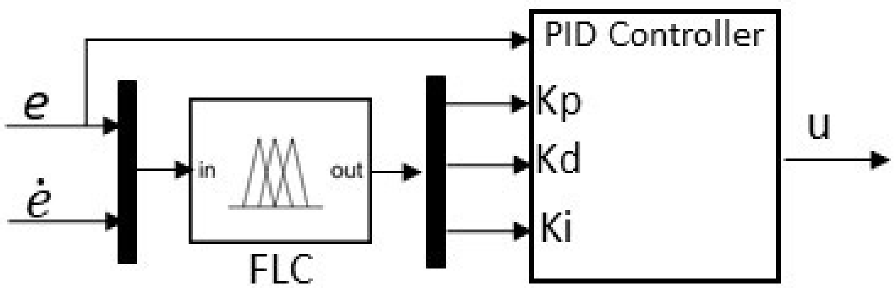

Figure 3.5 Gain Scheduling Type Fuzzy-PID Controller Structure

3.2.3 Hybrid Type Fuzzy-PID Controller

The hybrid Fuzzy-PID controller is set up by joining of a double-input direct type fuzzy PID controller and conventional PID controller. Controller diagram representation is indicated in Figure 3.6.

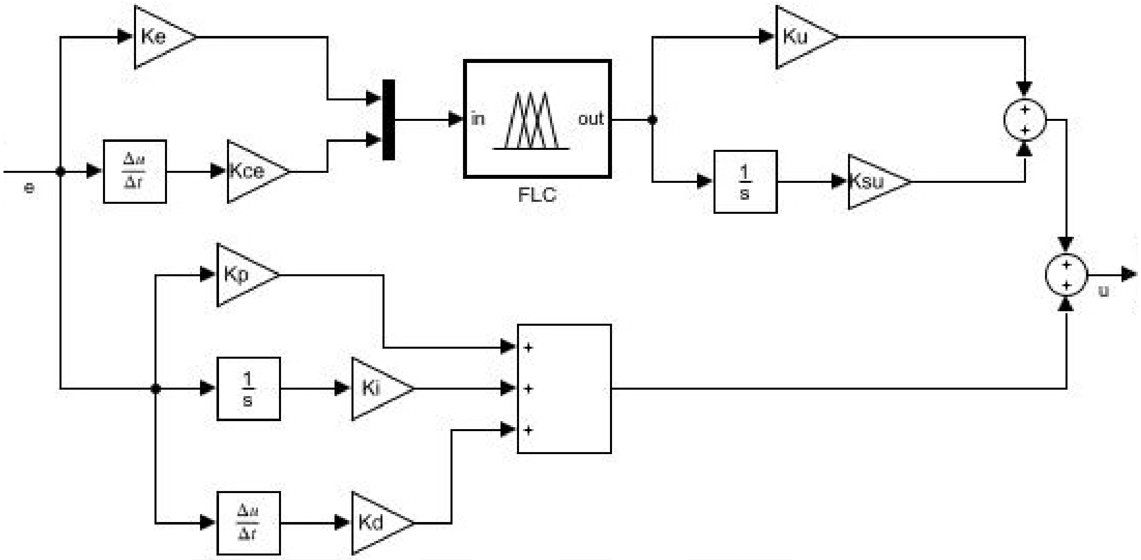

Figure 3.6 Hybrid Type Fuzzy-PID Controller Structure

3.3 Implementation of Controller and Energy Management Strategy

In this chapter, it will be issued how energy management algorithm is implemented and how controller is integrated into the system. Entire vehicle system is combined to double input Fuzzy-PID type controller and optimized controller gains are identified by BBBC algorithm where the cost as function of vehicle speed error and consumed fuel rate [L/100km] is minimum. With found fuzzy-PID controller parameters, simulation is performed once again, and result are discussed in Chapter 4. How system released in Figure 3.7 is working without BBBC optimization method can be explained that Fuzzy-PID controller firstly checks square of error as gap between speed reference and actual vehicle speed which is feedback from powertrain system then it releases required either traction or brake torque rate signal of driver demand. Traction torque demand is proportional rate of gas pedal. Lastly, demanded torque is captured by hybrid control system and it defines torque split between engine and motor based aligned algorithms and powertrain elements' toque is sent to powertrain system block to feed vehicle propulsion.

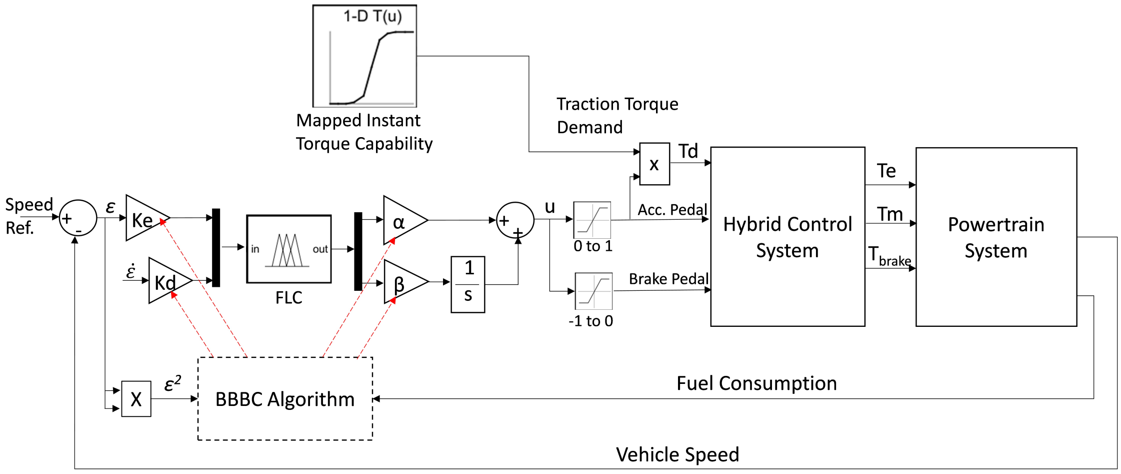

Figure 3.7 Fuzzy-PID Controlled System

Sugeno type fuzzy inference introduced in 1985 [30] is used as output membership function is constant and input-output membership functions are denoted in Figure 3.8 where N is Negative; NM is Negative Medium; Z is Zero; PM is Positive Medium; P is Positive. FLC properties der defined in MATLAB toolbox.

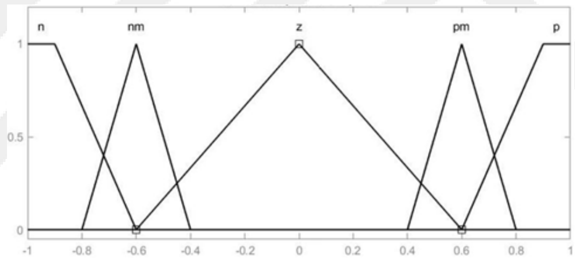

(a)

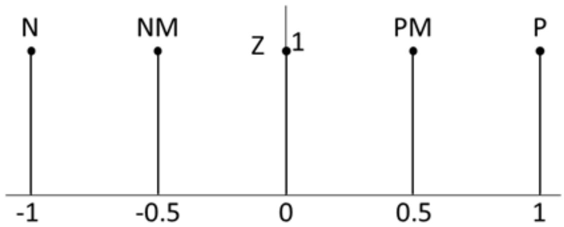

(b)

Figure 3.8 (a)Input MFs and (b) Output MFs

Since there are five membership functions of both inputs, controller has 25 rules and they are also given in Table 3.2.

Table 3.2 FLC rule table

e_dot\e	**N**	**NM**	**Z**	**PM**	**P**
N	N	N	NM	NM	Z
NM	N	NM	NM	Z	PM
Z	NM	NM	Z	PM	PM
PM	NM	Z	PM	PM	P
P	Z	PM	PM	P	P

3.4 PID Controlled Application

Same strategy and algorithm of BBBC like performed in fuzzy-PID controller is also applied to conventional-PID controlled model by defining new PID variables. Entire system block diagram is given in Figure 3.9.

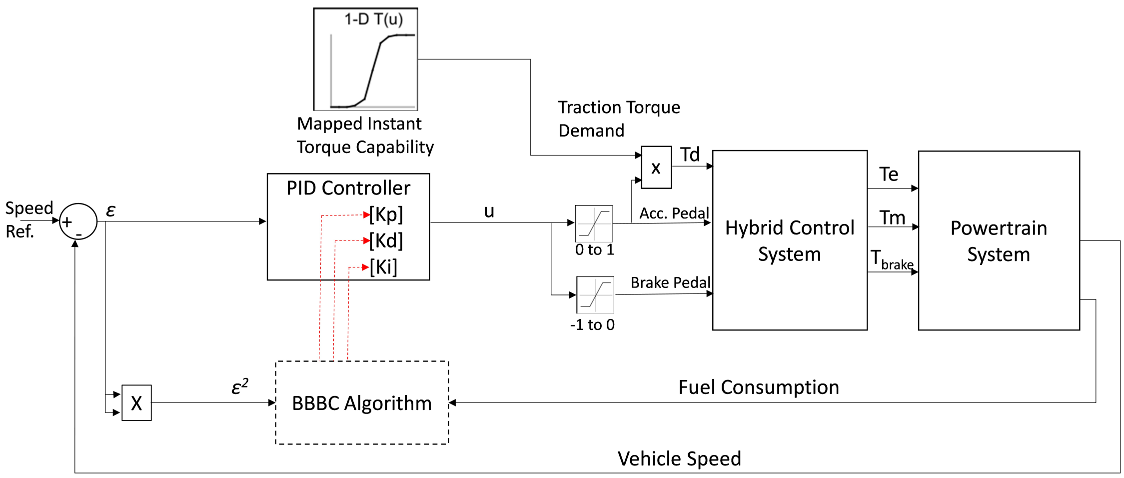

Figure 3.9 Conventional-PID Controlled System

4
Simulation Studies

In this chapter, simulation results applied to parallel hybrid electric passenger vehicles are indicated to clarify utilities of a new energy management strategy issued in chapter 3.

Main purpose of the thesis is to simulate a parallel hybrid electric passenger car to minimize vehicle fuel consumption value with comparison between conventional PID and Fuzzy-PID controller performance by utilizing 765 second-HWFET drive cycle as a reference. Total distance is calculated as 16.51 km.

This chapter includes two main sections to go through simulation results given as:

- Powertrain Elements condition during traction and braking on longitudinal vehicle dynamics,
- Applied optimization method performance for energy management.

Simulation assumptions are

- Road slope is 0,
- Wind speed is 0,
- Vehicle is cruising on flatted ground and straight road,
- Battery operating temperature is stable and is $25^{o}C$,
- Battery equivalent circuit contains voltage source (OCV) and internal resistance,
- Initial battery SOC is 50%.
- Motor efficiency is constant at every condition and is 90%,
- Auxiliary power consumption such as vehicle air conditioning, lighting is ignored,

- Engine brake and its inertia are not considered,
- Wheel has no slip on the road and wheel radius is implemented as constant during simulations,
- Clutch losses and dynamics are neglected,
- Gear transitions are smooth and there is no disturbance between transitions,
- Motor is considered as first power source and engine is in support position as long as battery SOC is higher than 20%,
- Hybrid traction mode, electric drive mode and regenerative braking mode are simulated by ignoring other modes like battery charging, only engine mode, etc.

4.1 Powertrain Elements Performance

This section explains battery, engine and motor performance results. It is seen in Figure 4.1 that values are inside motor torque limits [-120 120] for both controllers, however it seems C-PID values at some points is slightly exceeding torque value from F-PID data.

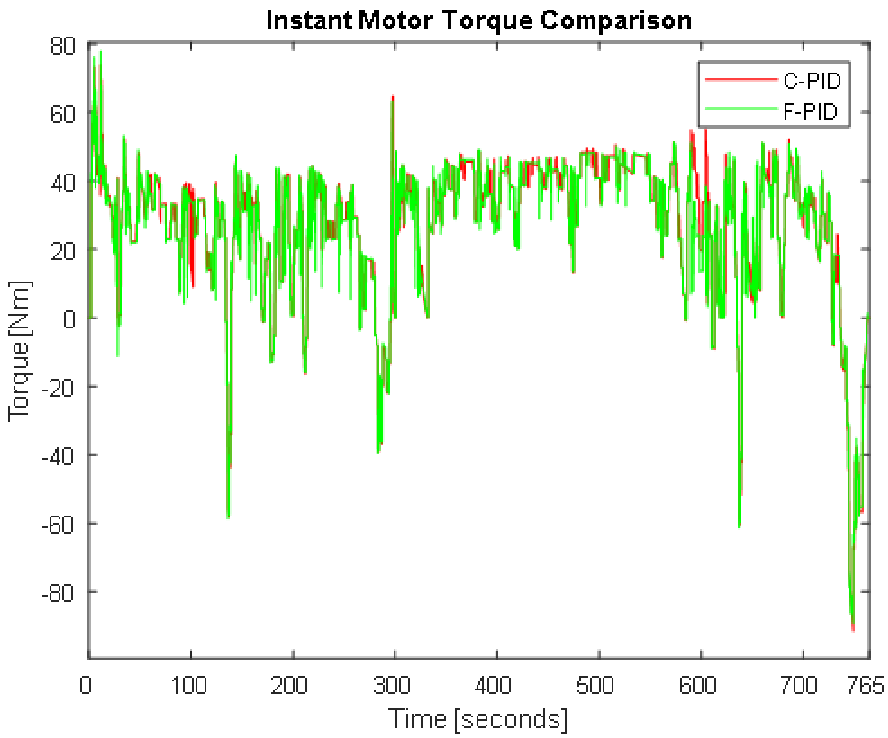

Figure 4.1 Actual Requested Motor Torque Value

As motor torque values indicated in Figure 4.1, it leads to consume much more battery energy in C-PID controller application because it applies higher torque value.

Therefore, it is seen Figure 4.2 that battery SOC rate reaches lower value in C-PID controller at the end of simulation. Besides, that also affects on having more current like illustrated in Figure 4.3.

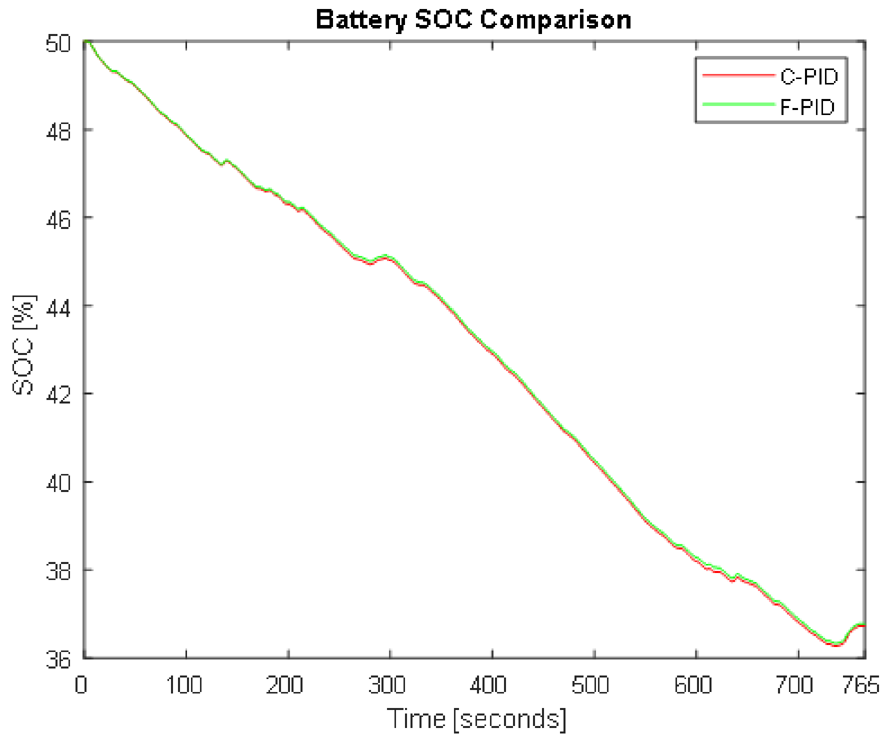

Figure 4.2 Actual Battery SOC

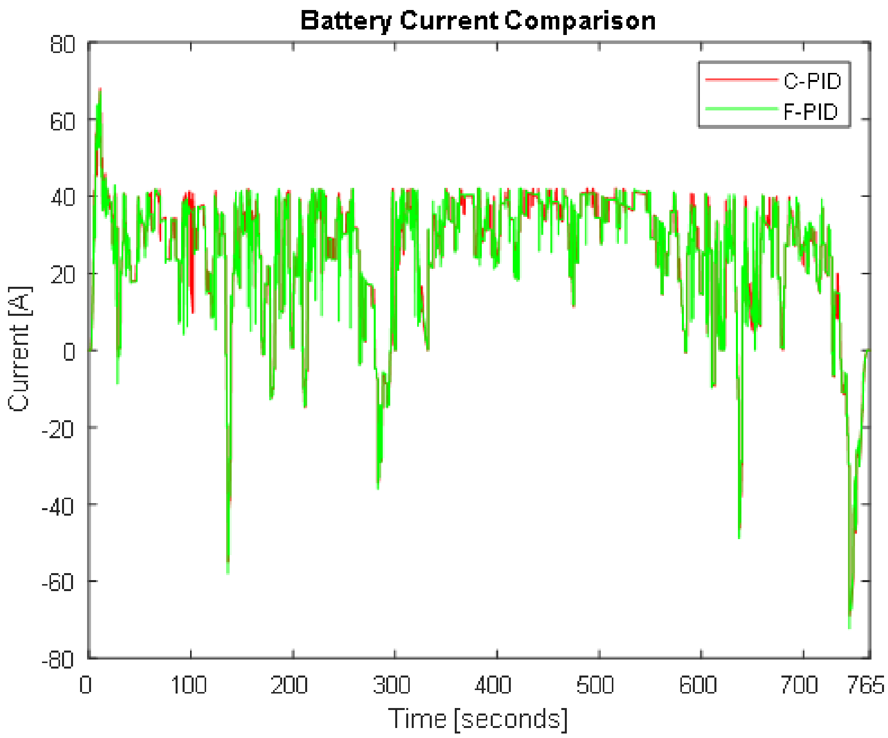

Figure 4.3 Drawn Battery Current

Figure 4.3 obviously indicates drawn battery current and instant motor power given in Figure 4.4 is similar to each other because vehicle auxiliary power is ignored during simulations. Generally, motor requires 40A and 10kW power continuously because of battery limit. If power demand by driver is higher than 10kW, then engine will handle remaining requested torque. As mentioned in previous chapters, Figure 4.6 illustrates engine torque is greater than 0 in minor points due to the fact that motor primary source of vehicle propulsion in relative battery limits.

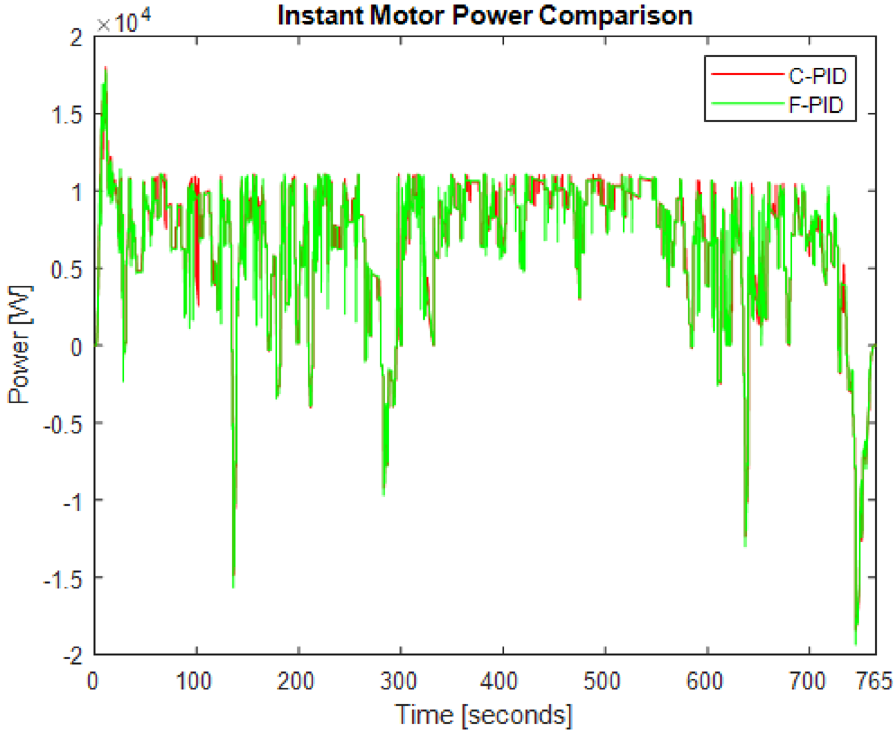

Figure 4.4 Actual Motor Power Value

Although engine torque is performed at very short duration like seen in Figure 4.5, it does not mean that engine is stop. In that conditions, engine is stand by status and clutch is engaged. However, engine torque is set to 0 and it is assumed that there is no fuel consumption. Comprehensive information about Engine status transition can be found in chapter 2, traction model. Therefore, how actual engine speed is issued can be found in Figure 4.6. Motor speed also draws same speed graph as clutch is nearly engaged in whole drive cycle.

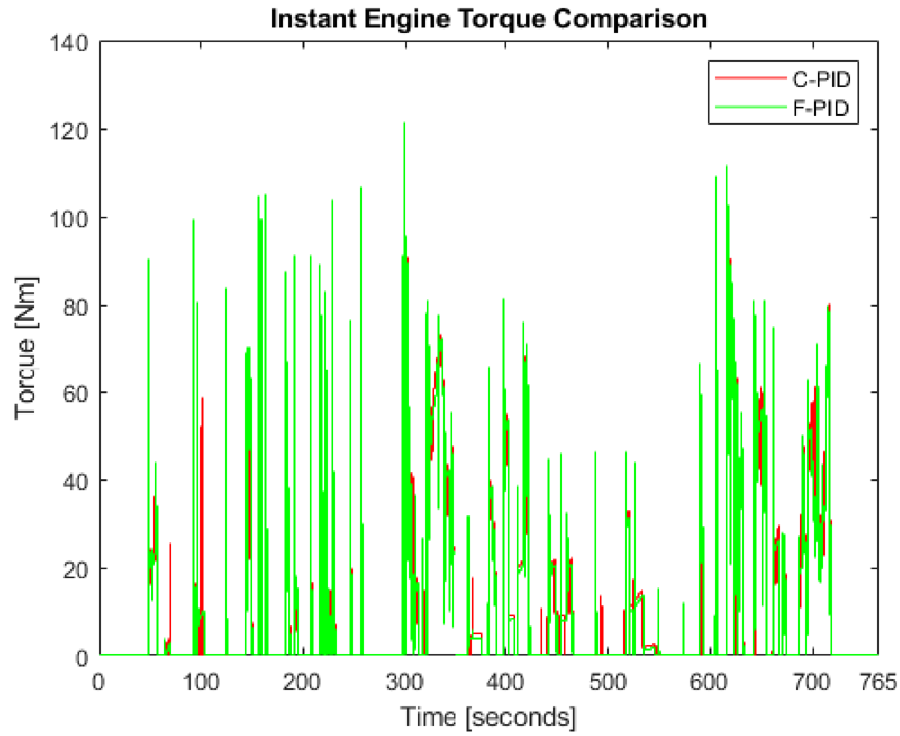

Figure 4.5 Actual Requested Engine Torque Value

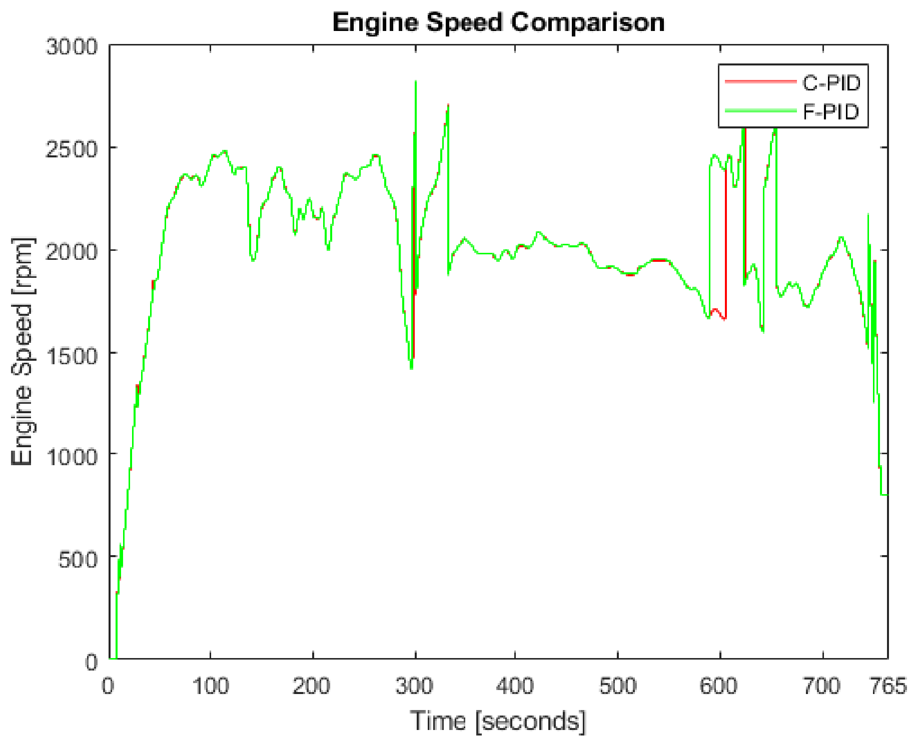

Figure 4.6 Actual Engine Speed

4.2 Optimization Performance

As it is defined in Chapter 3, BBBC optimization method is used for having minimum cost function demonstrated in equation (3.3) and obtained controller parameters based on BBBC algorithm in Appendix-A are given in Table 4.1.

Table 4.1 Optimized controller parameters

	F-PID				**C-PID**		
Gain	Ke	Kd	α	β	Kp	Kd	Ki
Value	3.6652	0.0356	0.9755	10.0652	9.6492	0.0425	0.7571

Table 4.2 summarizes that following figures. In addition, Table 4.2 shows that F-PID controlled system consumes 1.37 L/100km and C-PID controlled model releases 1.408 L/100km. That means fuel rate in F-PID system is decreased by 2.70% compared to C-PID controlled vehicle. Due low fuel mass in F-PID controller application, it also causes lower CO_2 emission rate by 2.72%.

Table 4.2 Consumed fuel and released emission rate

	Fuzzy-PID			**Conventional-PID**		
Parameter	Fuel Consump. [L/100km]	CO_2 Emission [g/km]	Final Battery SOC [%]	Fuel Consump. [L/100km]	CO_2 Emission [g/km]	Final Battery SOC [%]
Value	1.37	31.53	36.78	1.408	32.41	36.73

Figure 4.7 and Figure 4.8 are derived from mapped engine parameters based on instant engine rotational speed and torque. In summary, C-PID responses are usually exceeding required torque values in F-PID response and that leads to higher fuel and emission rate cumulatively while simulation is reaching to last seconds.

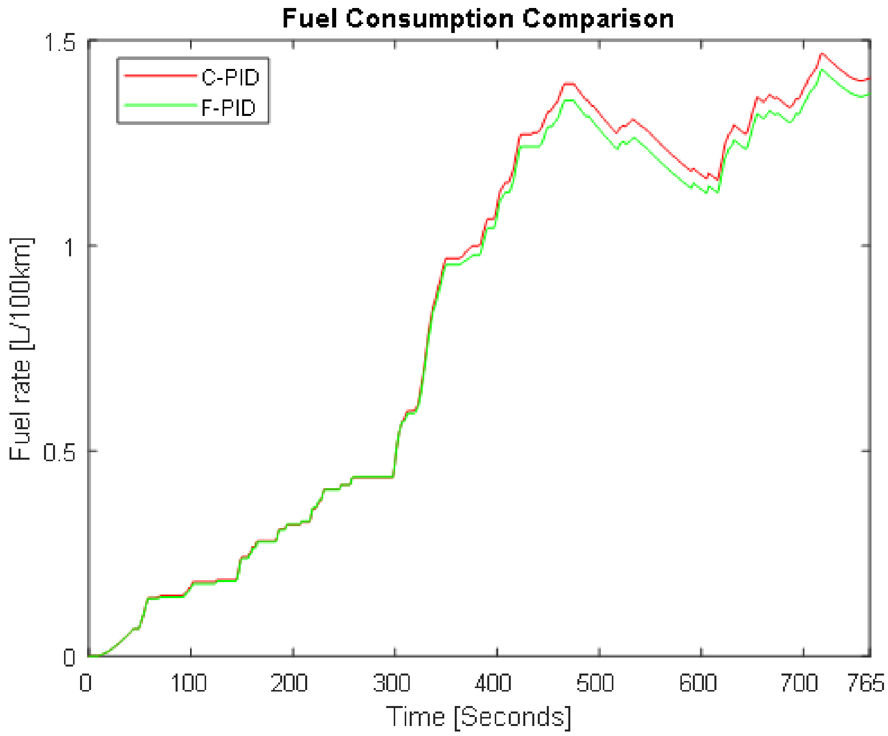

Figure 4.7 Consumed Fuel Rate

As CO_2 released compound once fuel is ignited, Figure 4.8 shows emission rate is proportionally higher like seen fuel consumption graph.

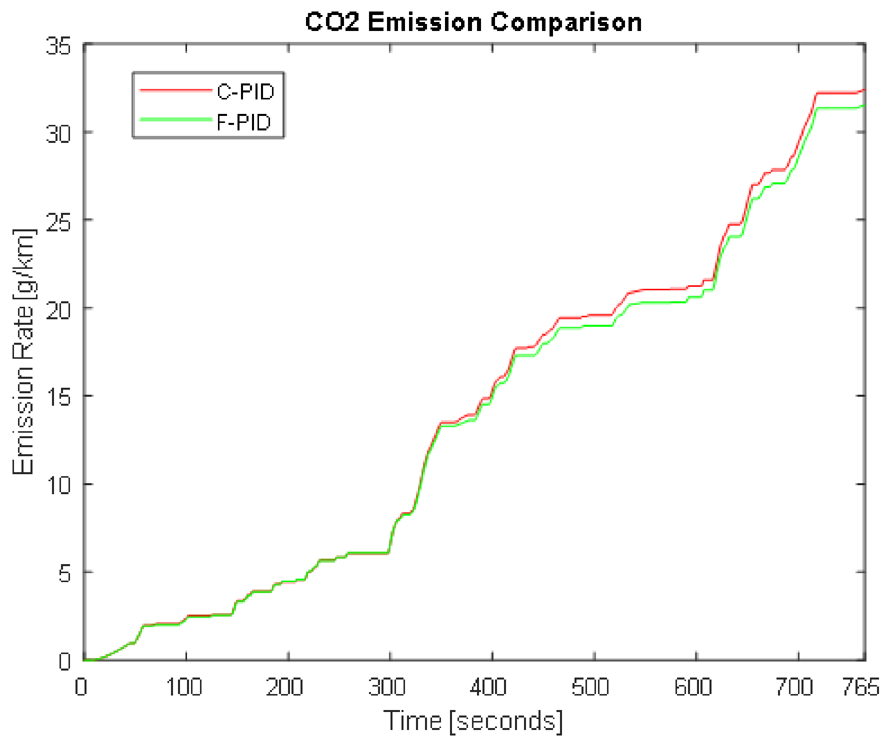

Figure 4.8 Released CO_2 Emission

Obviously, it is observed in vehicle speed result, vehicle follows given speed reference quite well. However, F-PID controller application refers to better results than C-PID. Due to the fact that vehicle speed and fuel rate in both controller application are very similar to each other, results refer to nearly same values.

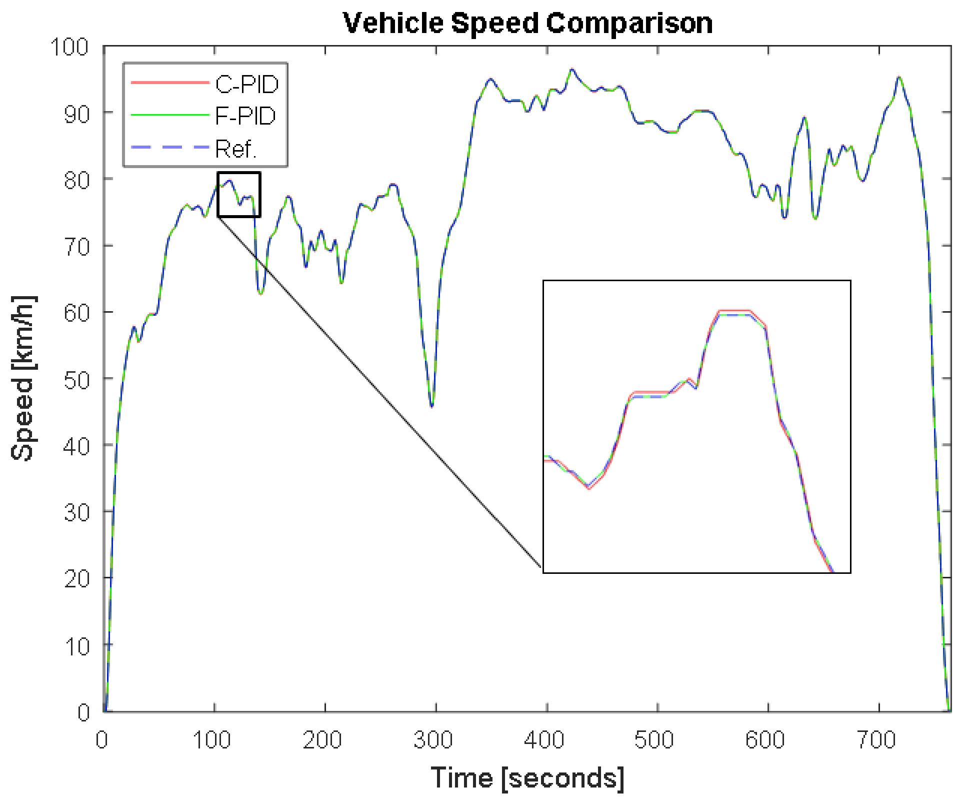

Figure 4.9 Vehicle Speed Reference and Actual Vehicle Speed for both Controllers

To summarize all simulation studies, it is realized that performance values are convenient with limits defined as specification in Chapter 2, Vehicle Model.

5
Results and Discussion

Main purpose of the thesis is to investigate a new energy management method performance to be applied in parallel type hybrid electric powertrain structure, as well as advancement of fuel consumption and emission rate.

In this thesis, a parallel hybrid electric passenger car is modeled and is discussed for optimized energy management. BBBC algorithm depended on speed error and fuel consumption has been applied as energy management strategy to gather optimum result for Fuzzy-PID and conventional PID gains. And then, the effect of both controllers on fuel rate, emission rate and the output of drivetrain components are reviewed and compared via MATLAB Simulink tool. The vehicle model is tested for only one drive cycle called as 765 second-HWFET.

Results indicate that Fuzzy-PID controller leads to better performance compared to classical PID in terms of fuel consumption, CO_2 emission and battery SOC. It concludes that F-PID controller is more robust than C-PID controller for modeled vehicle system.

A
BBBC Algorithm for Controller Coefficient

```
global variable1 %Assignment of new variable Ke,Kd,Kp…
global Variable2
global Variable3
global Variable4

n=Variable Count; %Number of variable Ke,Kd,Kp… n=4 for F-PID, n=3 for
C-PID
iteration=Number; %Defines how may times population is generated
popsize=Number; %Defines population cluster

upper=[Value,Value.Value,Value];   %upper bound
lower=[0.01,0.01,0.01];   %lower bound

for i=1:n  % Creating primary population
    pop(:,i)=(upper(i)-lower(i))*rand(popsize,1)+lower(i);  % Random
Individuals
end

for i=1:iteration
    for j=1:popsize
        variable1=pop(j,1);
        variable2=pop(j,2);
        variable3=pop(j,3);
        variable4=pop(j,4);

        sim('Model Name') % Start up related simulation
        cost(j)=Simulated_Cost(end);
    end
    pop=bbbcf(pop,cost,upper,lower,i);  % BBBC algorithm starts for
min cost function
end

pop(popsize,:)
Variable1=pop(popsize,1)  % optimum values are sent to Simulink
Workspace
Variable2=pop(popsize,2)
Variable3=pop(popsize,3)
Variable4=pop(popsize,4)

sim('Model Name') %Run simulation with optimum values lastly
cost(end)   %Record cost value
```

References

[1] U.S. Department of Transportation, ITS Research Archive, *http://www.its.dot.gov/research/vehicle-electrification-smartgrid.htm*, 5 January 2015

[2] S. F. Tie, C. W. Tan "*A review of energy sources and energy management system in electric vehicles*", Renewable and Sustainable Energy Reviews 20, 82-102, 2013

[3] Y. Gurkaynak, A. Khaligh, A. Emadi. "*State of the art power management algorithms for hybrid electric vehicles*", 978-1-4244-2601-0/09 IEEE., 2009.

[4] H.-D. Lee, E.-S. Koo, S.-K. Sul, J.-S. Kim, M. Kamiya, H. Ikeda, S. Shinohara, H. Yoshida. "*Torque control strategy for a parallel-hybrid vehicle using fuzzy logic*", IEEE Industry Applications Magazine, vol. 6, no. 6, pp. 33-38, Nov.-Dec. 2000.

[5] S. G. Li, S. M. Sharkh, F. C. Walsh, C. N. Zhang "*Energy and battery management of a plug-in series hybrid electric vehicle using fuzzy logic*", IEEE Transactions on Vehicular Technology, vol. 60, no. 8, pp. 3571-3585, Oct. 2011.

[6] S.D. Farrall, R.P. Jones. "*Energy management in an automotive electric/heat engine hybrid powertrain using fuzzy decision making*", Proceedings of 8th IEEE International Symposium on Intelligent Control, Chicago, IL, USA, pp. 463-468, 1993.

[7] P. Caratozzolo, M. Serra and J. Riera. "*Energy management strategies for hybrid electric vehicles*", IEEE International Electric Machines and Drives Conference, 2003. IEMDC'03., Madison, WI, USA, vol.1, pp. 241-248, 2018.

[8] X. Qi, G. Wu, K. Boriboonsomsin, M.J. Barth. "*Development and evaluation of an evolutionary algorithm-based online energy management system for plug-in hybrid electric vehicles*", IEEE Transactions on Intelligent Transportation System, vol. 18, no. 8, 2181–2191, 2017.

[9] A. A. Malikopoulos. "*Supervisory power management control algorithms for hybrid electric vehicles: a survey*", IEEE Transactions on Intelligent Transportation System, vol. 15, no. 5, 2014.

[10] C. Guardiola, B. Pla, S. Onori, G. Rizzoni. "*Insight into the HEV/PHEV optimal control solution based on a new tuning method*", Journal of Control Engineering Practice, Vol. 29, pp. 247-256, 2014.

[11] C.-C. Lin, H. Peng and J. W. Grizzle. "*A stochastic control strategy for hybrid electric vehicles*", Proceedings of the 2004 American Control Conference, Boston, MA, USA, vol.5, pp. 4710-4715, 2004.

[12] Z. Chen, C. C. Mi, R. Xiong, J. Xu, C. You. "*Energy management of a power-split plug-in hybrid electric vehicle based on genetic algorithm and quadratic programming*", J. Power Sour., vol. 248, no. 15,pp. 416–426, 2014.

[13] A. K. Yadav, P. Gaur. "*An optimized and improved STF-PID speed control of throttle controlled HEV*", Arab J Sci Eng. 41:3749–3760, 2016.

[14] A. Chasse, P. Pognant-Gros, A. Sciarretta. "*Online implementation of an optimal supervisory control for a parallel hybrid powertrain*", SAE International 2009-01-1868, 2009.

[15] C. Musardo, G. Rizzoni, Y. Guezennec, B. Staccia. "*A-ECMS: an adaptive algorithm for hybrid electric vehicle energy management*", European Journal of Control, Vol. 11, Issues 4–5, Pages 509-524, 2005.

[16] C. Liu,, Y. L. Murphey. "*Analytical greedy control and Q-learning for optimal power management of plug-in hybrid electric vehicles*", IEEE 978-1-5386-2726-6/17, 2017.

[17] C. Liu,, Y. L. Murphey. "*Power management for plug-in hybrid electric vehicles using reinforcement learning with trip information*", IEEE 978-1-4799-2262-8/14, 2014.

[18] C. C. Chan, A. Bouscayrol, K. Chen. "*Electric, hybrid, and fuel-cell vehicles: architectures and modeling*", IEEE Transactions on Vehicular Technology, vol. 59, no. 2, 2010.

[19] K. Erhan. "*Hibrit ve elektrikli araçlarda volan ve ultrakapasitör teknolojilerinin kullanımının incelenmesi ve volan enerji depolama ünitesinin prototip üretimi*", PhD Thesis, Kocaeli University, Graduate School of Natural and Applied Sciences, Kocaeli, 2018.

[20] T. Nüesch, A. Cerofolini, G. Mancini, N. Cavina, C. Onder, L. Guzzella. "*Equivalent consumption minimization strategy for the control of real driving NOx emissions of a diesel hybrid electric vehicle*", Energies 2014, 7, 3148-3178., 2015.

[21] MathWorks Disc Brake Description.
https://www.mathworks.com/help/physmod/sdl/ref/discbrake.html.

[22] A. Seamana, T. Daob, J. McPheea. "*A survey of mathematics-based equivalent-circuit and electrochemical battery models for hybrid and electric vehicle simulation*", Journal of Power Sources, vol. 256, pp. 410-423, 2014.

[23] J. Zhang, J. Lee. "*A review on prognostics and health monitoring of Li-ion battery*", Journal of Power Sources, vol. 196, no. 15, pp. 6007-6014, 2011.

[24] J. Peng, H. Fan, H. He, D. Pan. "*A rule-based energy management strategy for a plug-in hybrid school bus based on a controller area network bus*", Energies 2015, 8, 5122-5142, 2015.

[25] N. A. Samad, Y. Kim, J. B. Siegel, A. G. Stefanopoulou. "*Influence of battery downsizing and SOC operating window on battery pack performance in a hybrid electric vehicle*", IEEE Vehicle Power and Propulsion Conference (VPPC), 2015.

[26] O. K. Erol, İ. Eksin. "*A new optimization method: Big Bang–Big Crunch*", IEEE Vehicle Power and Propulsion Conference (VPPC), Advances in Engineering Software, Vol. 37, no. 2, pp. 106-111, 2006.

[27] A. Ersöz. "*Büyük patlama büyük çöküş optmizasyon algoritması tabanlı bulank modelleme yöntemi ve yazlımı*", MSc Thesis, Istanbul Technical University, Graduate School of Natural and Applied Sciences, Istanbul, 2011.

[28] T. Kumbasar, E. Yesil, I. Eksin and M. Guzelkaya. "*Inverse fuzzy model control with online adaptation via big bang-big crunch optimization*", 3rd International Symposium on Communications, Control and Signal Processing, St Julians, pp. 697-702, 2008.

[29] B. Akbıyık, İ. Eksin, M. Güzelkaya, E. Yeşil. "*Evaluation of the performance of various fuzzy PID controller structures on benchmark systems*", ELECO ’2005, 4rd International Conf. on Electrical and Electronics Engineering, Bursa, Turkey, 2005.

[30] M. Sugeno. "*Industrial applications of fuzzy control*", Elsevier Science Pub. Co., 1985.

[31] M. H. Amoozgar, A. Chamseddine, Y. Zhang. "*Fault-tolerant fuzzy gain-scheduled PID for a quadrotor helicopter testbed in the presence of actuator faults*", IFAC Proceedings Volumes, vol. 45, no. 3, 2012, pp. 282-287, 2012.